Chem Soc Rev

REVIEW ARTICLE

Covalent Post-Assembly Modification in Metallosupramolecular Chemistry

Derrick A. Roberts, Ben S. Pilgrim and Jonathan R. Nitschke*

Received 00th January 20xx,
Accepted 00th January 20xx

DOI: 10.1039/x0xx00000x

www.rsc.org/

A growing variety of covalent reactions have been employed to achieve the post-assembly modification (PAM) of self-assembled metallosupramolecular complexes. Covalent PAM enables the late-stage derivatisation of pre-assembled parent complexes in a modular fashion, thus expanding the chemical space available for supramolecular synthesis. The oldest and most widespread implementation of covalent PAM is in metal-preorganised covalent synthesis. Recent work, however, has broadened the scope of covalent PAM to include: protocols for efficiently grafting new functionalities onto supramolecular architectures, reactions that permanently 'lock-down' metastable complexes, and covalent bond-forming stimuli that trigger controlled structural transformations between distinct supramolecular species. This review highlights key examples of each of these distinct kinds of covalent PAM in metallosupramolecular chemistry, before providing a perspective upon future challenges and opportunities.

Introduction

Coordination-driven self-assembly has been developed into one of the most useful and versatile pillars of modern supramolecular chemistry.[1] The rich coordination chemistry of transition metals and the variety of available organic ligands have provided access to many two- and three-dimensional metallosupramolecular complexes that are both beautiful and useful.[2]

The construction of a metallosupramolecular complex requires a combination of covalent organic synthesis and coordination-driven self-assembly. Stepwise organic reactions are initially used to craft the constituent ligand building blocks of the complex. Subsequent metal coordination self-assembly equilibria then bring these building blocks into a higher-order architecture. For most metallosupramolecular structures, the use of organic chemistry is confined to pre-assembly ligand synthesis. Consequently, the assembled complex can only carry functional groups that are already present on the ligand building blocks. However, there is a growing collection of complexes that are amenable to covalent *post-assembly modification* (PAM) reactions, enabling the introduction of new functionality to a complex *after* it has formed.

PAM reactions are widespread in biology, particularly in the form of protein post-translational modification (PTM)[3] and the epigenetic modification of DNA.[4] Such PAM reactions are critically important to normal cell function as they can regulate protein activity, direct where a protein is localised within subcellular environments, and alter how proteins interact with other biomacromolecules.[5] Inspired, in part, by the roles that these reactions play in biology, analogous post-synthetic modification reactions have become widespread tools for the late-stage derivatisation of polymers,[6] metal-organic frameworks (MOFs),[7] and covalent-organic frameworks (COFs).[8] In these contexts, post-synthetic modification not only enables rapid and modular diversification of parent compounds, but also offers a way to overcome functional group incompatibilities that would otherwise interfere with the formation of a compound.

While covalent PAM of discrete metal–organic complexes can also be useful in metallosupramolecular chemistry, it has received significantly less attention than the post-synthetic modification of polymers, MOFs, and COFs. This lack of attention results from the more fragile and dynamic nature of self-assembled coordination complexes, which poses distinct challenges to performing covalent bond-forming reactions. For example, discrete metallosupramolecular complexes may decompose if exposed to incompatible reagents, including strong nucleophiles and electrophiles, highly coordinating species, or oxidising/reducing agents.[9] Furthermore, purifying mixtures of supramolecular complexes can be challenging because they may decompose at high dilution and often adhere irreversibly to chromatographic stationary phases. To be useful, a PAM reaction must be highly efficient (ideally quantitative), not interfere with metal–ligand coordination interactions, and should proceed under mild conditions. Fortunately, several covalent bond-forming methods—especially those classified as 'click'[10] reactions—satisfy these stringent requirements and have been successfully employed for the PAM of metallosupramolecular complexes.

Covalent PAM in metallosupramolecular chemistry draws upon essential early work by Jean-Pierre Sauvage in the early 1980s on the metal-preorganised covalent synthesis (MPCS) of mechanically-interlocked molecules—work that was subsequently recognized by the Nobel Committee for Chemistry

[a] Department of Chemistry, Lensfield Road CB21EW, University of Cambridge, United Kingdom. E-mail: jrn34@cam.ac.uk

in 2016.[11] In the first section of this review we briefly reflect upon this pioneering work and discuss selected examples that highlight the state-of-the-art in MPCS for generating complex molecular topologies. However, since this area of PAM has been the subject of several comprehensive recent reviews,[12] we focus our discussion on innovative uses of covalent PAM that have surfaced over the past 5-10 years. We divide this literature into three categories based on the purposes that covalent PAM serves: firstly, modular late-stage derivatization of supramolecular complexes; secondly, covalent reactions that kinetically "lock-down" dynamic supramolecular structures or "unlock" less labile ones; and thirdly, the use of covalent stimuli to trigger supramolecular structural transformations through *in situ* changes to the building block geometries.

We have restricted our discussion to reactions that occur exclusively on assembled complexes and not on the free building blocks, as far as can be demonstrated. Excluded thus, are building block (i.e., ligand/metal) exchange reactions, which necessarily proceed *via* at least partial framework dissociation, and reactions that break metal–ligand coordination bonds. Additionally, only PAM reactions that result in the introduction of new covalent bonds to the structure or, in the case of some PAM-locking approaches, act directly upon existing covalent bonds within the structure, are discussed. Since non-dynamic covalent bond formation is our focus, we omit detailed discussion of PAM using dynamic covalent chemistry (such as the exchange of imines, hydrazones, disulfides, acetals, orthoesters etc.), which is reviewed in detail elsewhere.[12b, 13] We instead focus on the separate challenge of selective covalent bond formation in reactions that are not spontaneously reversible under ambient conditions.

We hope this treatment of the literature will not only provide an overview of recent advances in this area, but also may help to frame perspectives for future areas of research.

1. Metal-preorganised covalent synthesis

In 1983, Sauvage and co-workers provided a canonical example of covalent post-assembly modification by describing the first synthesis of a [2]-catenane *via* the coordination of reactive precursors (**1** and **2**) around a Cu^{I} template (Figure 1).[14] The metal template holds the ligand building blocks in a geometry that is unlikely to be otherwise populated in bulk solution (complex **3**). Williamson ether synthesis was utilised to form new covalent bonds around the self-assembled complex, fixing the geometry such that interlocked structure **4** persisted upon removal of the metal template. In this way, geometric pre-organization of the building blocks enabled the formation of covalent bonds in a configuration that would be challenging or impossible to achieve using conventional covalent synthetic techniques. This early example of covalent PAM seeded many imaginations, resulting in the formation of a multitude of topologically-complex molecular architectures,[15] of which we highlight a few recent examples.

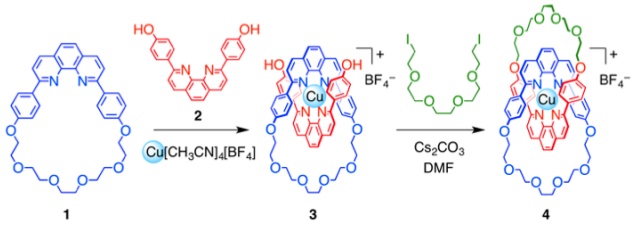

Figure 1. Sauvage's pioneering template synthesis of [2]-catenane **4** *via* the coordination of a Cu^{I} template to phenanthroline units **1** and **2**, followed by post-assembly Williamson etherification to mechanically interlock both macrocycles.[14]

Hunter and co-workers employed a carbodiimide-mediated esterification reaction to connect the two pendant primary alcohols on a zinc overhand knot complex (**5**) to form a trefoil knot (**6**) (Figure 2).[16] These authors also showed in the same study that ring-closing olefin metathesis (RCM) with Grubbs' First Generation catalyst could be used to tie two terminal alkenes in a similar manner.

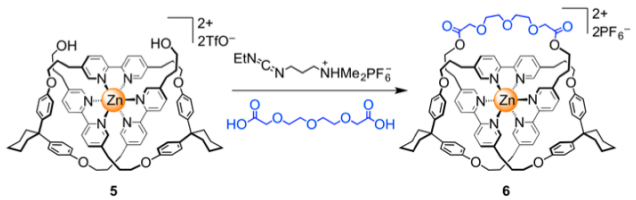

Figure 2. Hunter and co-workers' trefoil knot, **6**, formed by tying together the two pendant alcohols at the end of the overhand knot **5** using a dicarboxylic acid linker.[16]

Indeed, the olefin metathesis reaction has served as perhaps the most versatile PAM reaction for the synthesis of mechanically interlocked molecules and complex molecular topologies.[17] Several recent examples from the Leigh group highlight the state-of-the-art in this field. The coordination of six tris(2,2'-bipyridine) strands to six Fe^{II} centres gives hexameric circular helicate **7** (Figure 3a).[18] At the terminus of each strand is a phenyl ring bearing an *ortho*-substituted terminal alkene moiety. Each phenyl ring is twisted out of the plane of the adjacent bipyridine group due to steric hindrance, which brings alkene groups on adjacent ligands into proximity. Subjecting **7** to RCM using the Hoveyda–Grubbs second-generation catalyst furnished complex **8**. After RCM, the Fe^{II} ions could be removed, furnishing a fully organic [2]-catenane, consisting of two triply-entwined 114-membered rings in a 'Star of David' shape.

The Leigh group also found that the same tris(2,2'-bipyridine) strands could form pentameric circular helicate **9** (Figure 3b) rather than hexameric helicate **7** by altering the conditions during self-assembly.[19] Pentameric helicate **9** is always templated by a central Cl^- ion (scavenging one during synthesis when no specific source of Cl^- is added). RCM of **9** gave pentafoil knot **10**, which exhibits extremely strong binding of both Cl^- and Br^- (>1 × 10^{10} M^{-1} in CH_3CN).

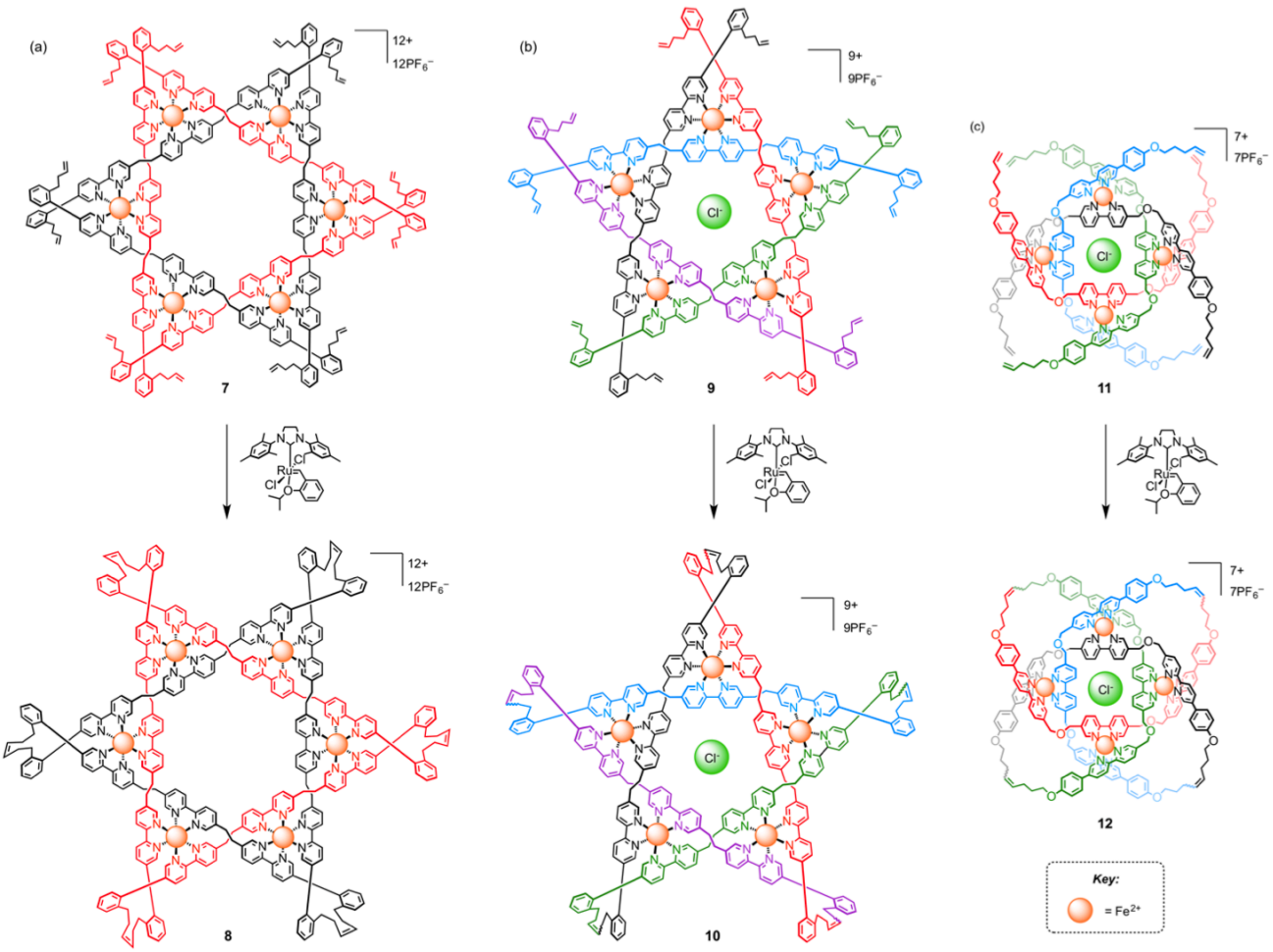

Figure 3. The Leigh group's use of ring-closing metathesis with the Hoveyda–Grubbs second-generation catalyst to access topologically-complex interlocked structures including (a) 'Star of David' [2]-catenane **8**,[18] (b) pentafoil knot **10**,[19] and (c) '8_{19}' molecular knot **12**.[20]

Following RCM, the ten Fe^{II} ions in **10** could undergo exchange for Zn^{II} ions. The zinc pentafoil knot also bound halides strongly, but the demetallated form of the knot did not. This zinc knot was shown to extract bromide from trityl bromide to give a tritylium ion, which in turn functioned as a Lewis acid catalyst in the Michael addition or Diels-Alder reactions of acrolein. Hence, it was possible to allosterically regulate catalysis of these reactions by the addition or removal of zinc (using Na_4EDTA) from the pentafoil knot.

Most recently, Leigh and co-workers showed that the coordination of four slightly more flexible tris(2,2'-bipyridine) strands to four Fe^{II} ions gave cyclic triple helix **11**, which is stabilised by a centrally-bound Cl^- ion.[20] RCM of the pendant alkenes generated triple-stranded molecular knot **12**. Known as the '8_{19}' due to its eight crossing points, and with a crossing every 24 atoms, **12** is the among the most tightly knotted synthetic objects.

In their studies of oligo-porphyrins, Anderson and co-workers discovered that the coordination linkages between pyridine templates and zinc porphyrins were sufficiently robust to tolerate Glaser-type couplings as a method of PAM. The principle of Vernier templation was used to access large rings more readily than with conventional template strategies.[21] The combination of components with different numbers of binding sites (oligo-porphyrin building block **13** with four binding sites, and pyridine template **14** with six binding sites) principally led to the formation of a 3:2 complex with 12 porphyrin units, as 12 is the lowest common multiple of four and six. Templation held the terminal alkynes on adjacent units of **14** in close enough proximity for them to be oxidatively coupled, generating 12-porphyrin ring complex **15**. After coupling, the pyridine templates were removed to give the free nanoring. This strategy was subsequently extended to the synthesis of larger rings with up to 40 porphyrin units,[22] longer linear oligo-porphyrins,[23] and a 12-porphyrin nanotube.[24]

The use of metal ions exclusively as geometric templates to facilitate mechanical bond formation has come to be known as 'passive templation'. A recent development in MPCS is the dual use of metal ions as both structural templates *and* catalysts to facilitate covalent bond formation—a strategy called 'active templation'. The catalytic abilities of certain metal templates (e.g., Cu^I, Ni^{II} and Pd^{II}) can mediate a wide range of covalent bond-forming reactions, which has led to elegant syntheses of various rotaxanes and catenanes.[25] This area has been reviewed

recently by Denis and Goldup, whence we direct readers for further discussion.[26]

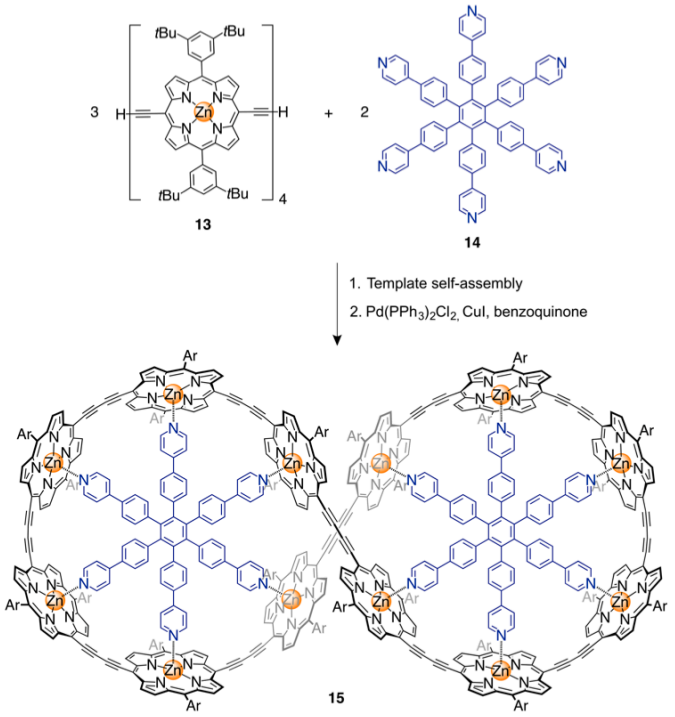

Figure 4. The Anderson group's use of Vernier templation to access a 12-porphyrin nanoring (**15**) through post-assembly Glaser-type coupling reactions.[21]

2. Modular derivatisation by covalent PAM

Covalent PAM is becoming increasingly useful for attaching new functional groups onto modifiable supramolecular complexes to generate diverse product libraries. A modular post-assembly approach to derivatisation can facilitate rapid screening for desired properties while avoiding the need for extensive pre-assembly ligand synthesis. Additionally, late-stage derivatisation can endow complexes with functional groups that are incompatible with self-assembly reactions, typically due to interference with metal-ligand bond formation during self-assembly (Figure 5). The development of diverse and robust PAM protocols thus makes it possible to rapidly increase the complexity of a parent complex.

There are few examples of self-assembled metal-organic architectures that feature reactive sites suitable for carrying out PAM. Care must be taken to ensure compatibility between these reactive sites and the metal-ligand bonds that hold together the assembled structure. Failure to do so can lead to decomposition of the parent assembly, or produce intractable mixtures of partially-functionalised supramolecular fragments.

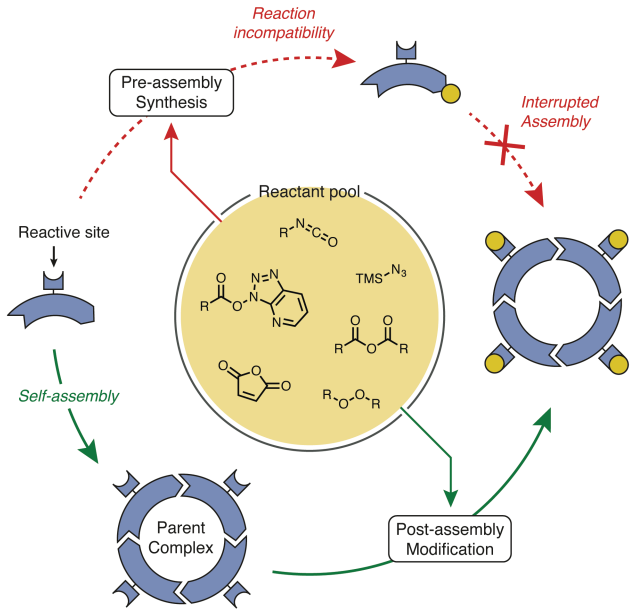

Figure 5. Reactive functional groups present on ligand building blocks facilitate pre-assembly synthesis and post-assembly modification (PAM) reactions. PAM is an invaluable tool when pre-assembly synthesis is unfeasible, such as when the ligands cannot be functionalised selectively, or when the introduced functional groups would interfere with assembly of the target complex.

Many of the reactions that have come to be called 'click reactions' work well for PAM due to their wide functional group tolerances and ability to proceed under mild reaction conditions. For example, Zhao *et al*. demonstrated PAM of cuboctahedron **16**, comprised of 12 dicopper(II) paddlewheel clusters and 24 5-(prop-2-ynyloxy)isophthalic acid units, *via* the copper-catalyzed azide-alkyne Huisgen cycloaddition (CuAAC) reaction (Figure 6).[27] Instead of employing the widely-utilised $Cu^{II}SO_4$/sodium ascorbate catalyst, the authors used $[Cu^{I}(CH_3CN)_4]PF_6$ to avoid reduction of the Cu^{II} paddlewheels. Performing this reaction using an azide-terminated poly(ethylene glycol) (PEG) furnished a mixture of click-grafted polymer-cage conjugates functionalized with up to four PEG chains at 24 possible reaction sites (**17**), indicating a possible steric limit to higher polymer grafting densities.

Post-assembly PEGylation rendered the assembled complex soluble and stable in aqueous media, contrasting with the known instability of its constituent dicopper(II) paddlewheels in water.[28] It is unlikely that water-soluble PEGylated cuboctahedron **17** could be prepared *via* direct self-assembly since the dicopper(II) paddlewheels would not form in water. Moreover, the hindered structure of PEGylated 5-(prop-2-ynyloxy)isophthalic acid building block might disfavor assembly into the target structure. Thus, post-assembly PEGylation was used to generate a supramolecular product not accessible through direct thermodynamically-controlled self-assembly.

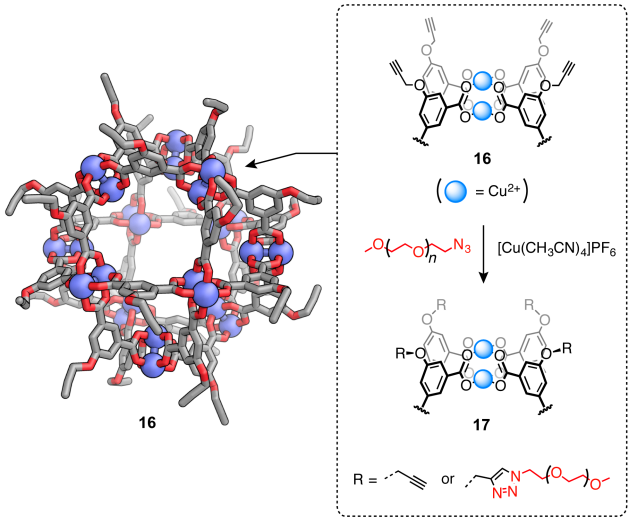

Figure 6. Zhao *et al.,* reported the synthesis of metal-organic cuboctahedron **16** from 5-(prop-2-ynyloxy)isophthalic acid, which was converted into polymer-cage conjugate **17** upon treatment with an azide-tagged PEG chain (1 equiv. per alkyne) under CuAAC conditions.[27] Steric congestion around the grafting sites reduced the efficiency of the CuAAC coupling reaction, affording **17** as a mixture of partially-coupled conjugates with up to four PEG chains per assembly. (Key for crystal structure: C = grey, O = red, Cu = blue. Coordinated solvent molecules have been omitted for clarity).

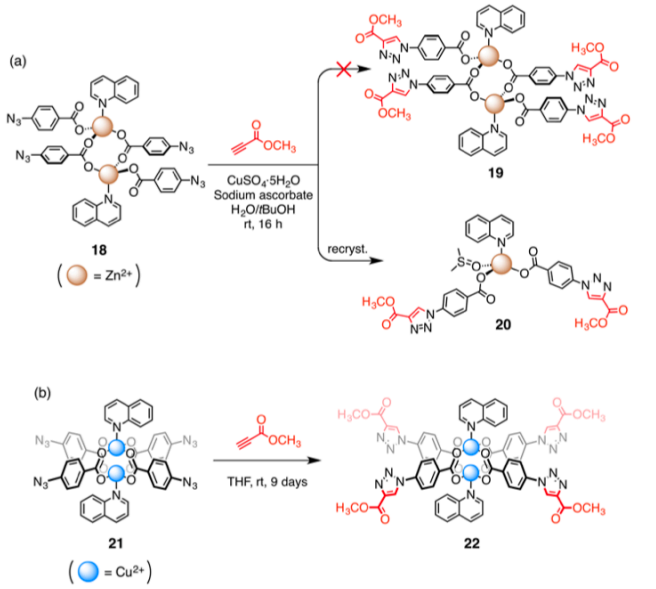

Figure 7. Potential incompatibilities must be taken into consideration when performing PAM reactions on metallosupramolecular complexes. (a) Moulton and co-workers found that dinuclear complex **18** decomposed under CuAAC conditions, failing to give the target complex (**19**).[29b] Recrystallisation of the crude product in the presence of quinoline revealed some triazole formation (**20**), but at the expense of the parent complex. (b) Using paddlewheel **21**, they found that the AAC reaction proceeded without Cu^{I} catalysis to give adduct **22** without decomposition.[29a]

Although generally mild, the CuAAC reaction can be unsuitable for the covalent PAM of particularly labile supramolecular complexes. For instance, Moulton and co-workers showed that a copper catalyst can interfere with labile metal-ligand bonds during the attempted modification of azide-bearing Zn^{II} and Cu^{II} complexes **18** and **21** (Figure 7).[29] The authors employed a Cu^{I} catalyst to avoid transmetallation. However, the use of $Cu^{II}SO_4$/sodium ascorbate also proved deleterious to the stability of complex **18**, resulting in decomposition to a mononuclear species, **20**, rather than formation of the target complex (**19**). The AAC reaction of Cu^{II} paddlewheel **21**, derived from the same ligand as **18**, was not attempted using the $Cu^{II}SO_4$/sodium ascorbate system due to the risk of reduction of the Cu^{II} paddlewheels. The authors overcame these complications by avoiding metal catalysis altogether, achieving clean conversion of paddlewheel **21** to the tetra(triazolyl) adduct (**22**) using an uncatalysed variant of the AAC reaction, which is known to proceed regioselectively under mild conditions when using electron-deficient alkynes.[30]

Despite its widespread use, the CuAAC reaction has limited biological applicability due to the cytotoxicity of its copper-based catalysts.[31] By contrast, the strain-promoted azide-alkyne cycloaddition (SPAAC) reaction,[32] originally developed by Bertozzi and co-workers,[33] circumvents the problem of cytotoxicity because it does not require a catalyst. Moreover, SPAAC is ideally suited to PAM since it involves weakly polarised reactants that minimize potential incompatibilities with metal-ligand coordination interactions.

Stang and co-workers thus developed a strategy for the PAM of self-assembled Pt^{II} metallacycles using the SPAAC reaction between azides and strained cyclooctynes.[34] Rhomboidal metallacycle **23** features two pendant cyclooctynyl units per complex, which undergo rapid and quantitative PAM when treated with organic azides. As a proof-of-concept, the authors demonstrated the attachment of a pyrene chromophore (**24**) and a biotin moiety (**25**) to the parent metallacycle. Considering the variety of two- and three-dimensional complexes that can be prepared from bis(pyridyl) building blocks[35] this strategy has promise as a general PAM strategy for different architecture types.

The tetrazine-based inverse electron-demand Diels-Alder (IEDDA) reaction is another cycloaddition reaction well suited for PAM. This reaction proceeds efficiently under mild conditions, produces only N_2 as an inert by-product, and is compatible with many dienophiles.[36] For these reasons, it has recently found use in the post-synthetic modification of polymers[37] and metal-organic frameworks,[38] and as a robust bioconjugation strategy for use in living tissue.[39]

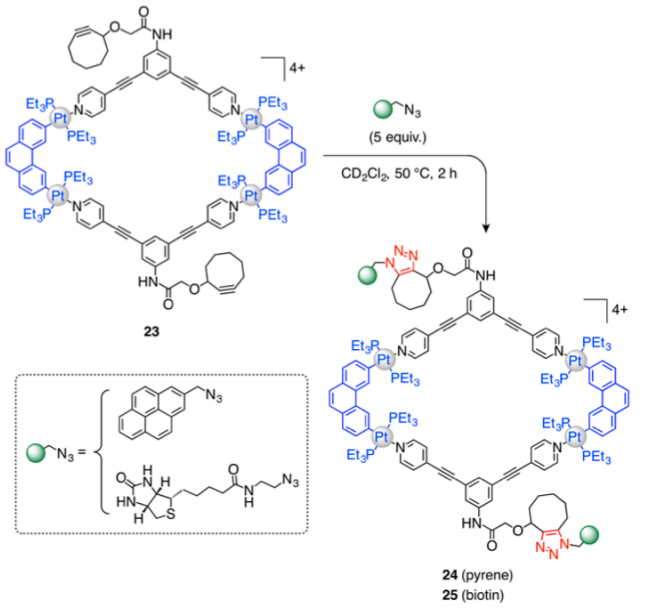

Figure 8. The incorporation of pendant cyclooctyne moieties onto metallacycle **23** enabled PAM using organic azides *via* the strain-promoted AAC reaction.[34] The wide range of commercially available azides and the scope for incorporating cyclooctynyl units into other assemblies opens avenues for future PAM studies.

In 2015, our group reported the use of tetrazine-based IEDDA reactions for the PAM of a discrete metallosupramolecular complex.[40] Congeners of tetrazine-edged $Fe^{II}_4L_6$ tetrahedron **26** underwent PAM reactions when treated with norbornadiene to give **27**, or more rapidly using the more reactive bicyclononylmethanol (BCNM) (1.4 equiv. per tetrazine) to give **28** (Figure 9). While norbornadiene did not endow **27** with additional functionality, BCNM offers myriad possibilities for attaching other functionalities *via* its pendant alcohol group. Although IEDDA reactions are known to proceed through distorted bicyclic intermediates,[36a] control experiments confirmed that **26** did not dissociate during the course of PAM, signalling its possible use as a general PAM strategy for other architectures derived from tetrazine-containing building blocks.

The design of the ligand framework within tetrahedron **26** engendered strong electronic coupling between the central tetrazine cores and the aniline residues incorporated at the vertices, through 11 bonds. This coupling manifested as a linear free energy relationship between the IEDDA rate constant and the Hammett σ parameter[41] of the aniline *para*-substituent: the more electron-withdrawing the substituent, the faster the IEDDA reaction.

In the tetrazine-norbornadiene IEDDA reaction, one equivalent of metastable cyclopentadiene is produced for every equivalent of norbornadiene consumed. Recognising that this reactive by-product could itself undergo a secondary PAM reaction, our group recently designed a reaction cascade comprised of sequentially-coupled PAM reactions.[42] Two cage architectures, tetrazine-edged $Fe^{II}_8L_{12}$ cube **29** and maleimide-functionalised $Fe^{II}_4L_6$ tetrahedron **30**, were designed to exhibit orthogonal Diels-Alder (DA) reactivities, whereby IEDDA on cube **29** produces a cyclopentadiene by-product that subsequently reacts with the maleimide units of tetrahedron **30** in a normal electron-demand DA reaction.

The addition of a trigger molecule (2-octadecylnorbornadiene) to an equimolar mixture of **29** and **30** initiated a cascade (Figure 10), culminating in the formation of pyridazine-edged cube **31** and tetrahedron **32**. Importantly, tetrahedron **32** arises from the selective alkylation of parent complex **30** *via* a transient 2-octadecylcyclopentadiene relay. Complete functionalisation of all twelve maleimide sites rendered tetrahedron **32** sufficiently lipophilic to cross a phase boundary from the polar acetonitrile reaction phase to a non-polar cyclopentane extraction phase. Tetrahedron **32** and its encapsulated PF_6^- cargo could thus be separated from cube **31**. The system thereby functionally mimics covalent post-translational modification reactions in natural systems, which form the basis of elaborate biological signalling cascades that allow information to be relayed from a microscopic triggering signal to produce a macroscopic output.

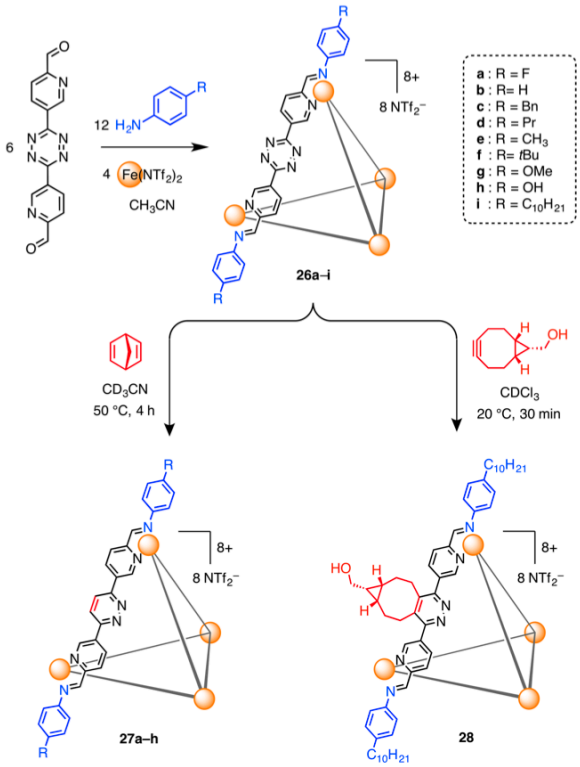

Figure 9. PAM on the central part of the ligand framework of tetrazine-edged tetrahedra **26a–i** was influenced by the electron richness of the peripheral aniline substituent during IEDDA to give **27a–h** upon treatment with NBD (2 equiv. per tetrazine).[40] PAM using BCNM (1.4 equiv. per tetrazine) gave **28**, which featured an alcohol group that permits further conjugation reactions.

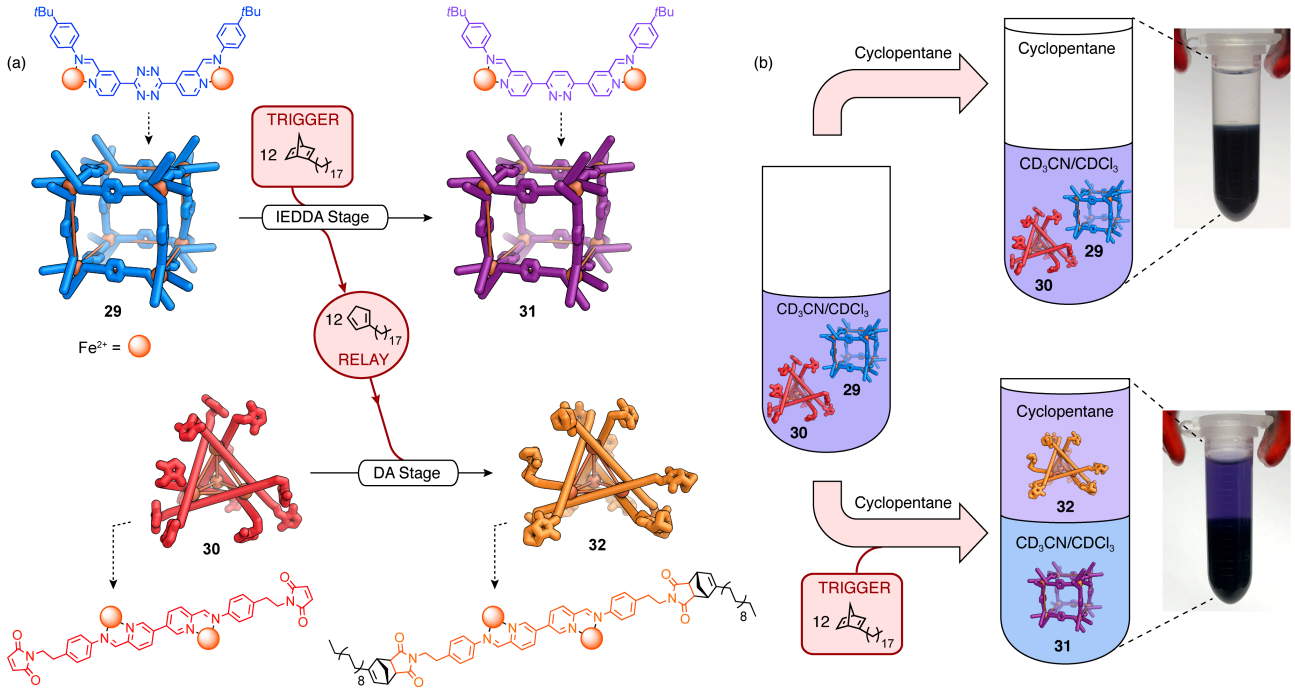

Figure 10. A cascade PAM sequence featuring an initial IEDDA reaction between 2-octadecylnorbornadiene and the tetrazine edges of cube **29**, followed by a DA reaction between 2-octadecylcyclopentadiene and the maleimide moieties of tetrahedron **30**.[42] Selective alkylation of tetrahedron **32** drives its partitioning into cyclopentane, allowing it to be isolated from cube **31**, which remains in the polar $CD_3CN/CDCl_3$ phase.

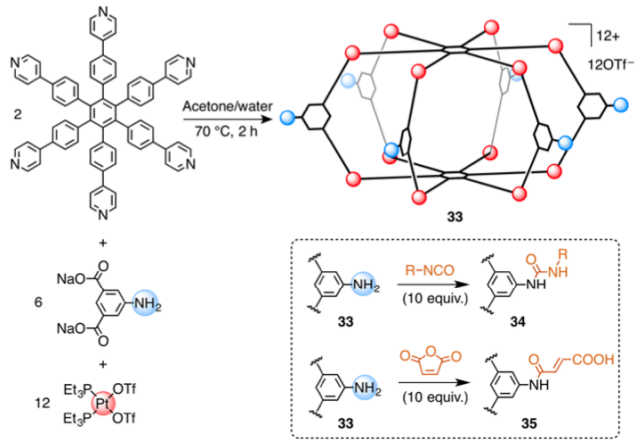

Figure 11. Self-assembly of $Pt_{12}L_6L'_2$ heteroleptic hexagonal prism **33**, which features six nucleophilic amine groups at its periphery.[43] The use of Pt^{II} vertices, which preferentially form heteroleptic complexes with pyridyl and carboxylate donors, ensures that the reactive amines do not interfere with the coordination bonds holding the prism together, thus allowing **33** to be modified by nucleophilic PAM reactions with primary isocyanates and maleic anhydride.

The use of AAC and IEDDA reactions for PAM is motivated in part by the weak polarisation of the reaction partners, which reduces the likelihood of incompatibilities with metal-ligand coordination motifs. Metal coordination does not, however, preclude the use of nucleophilic and electrophilic reagents in PAM strategies. For example, Stang and co-workers reported the successful functionalisation of an amine-bearing $Pt_{12}L_6L'_2$ heteroleptic hexagonal prism (**33**) using amine-isocyanate and amine-maleic anhydride nucleophilic addition reactions (Figure **11**).[43] The propensity of Pt^{II} to take two pyridyl and two carboxylate donors, and the slow rate of ligand exchange, ensures that the nucleophilic groups of the ligands remain tightly coordinated to the metal centres, even in the presence of electrophilic reagents. Consequently, PAM reactions proceeded cleanly to give the hexa-functionalised products **34** and **35**. In the case of **35**, the carboxylate group is necessarily introduced by PAM, since it would compete with the benzoate moieties for coordination to Pt^{II} if present on the dicarboxylate building block during self-assembly.

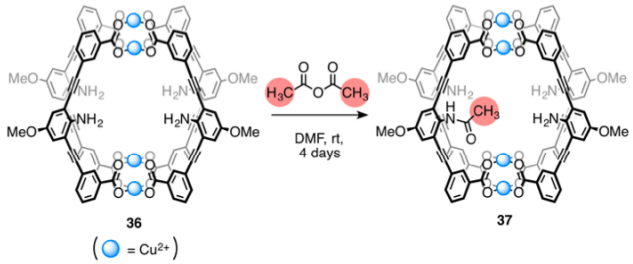

Figure 12. Cage **36** features four endohedral amine groups within its cavity. Treatment of **36** with excess acetic anhydride in DMF gave only monoacetylated complex **37**.[44] The small size of the cavity within **36** can accommodate the steric bulk of only a single acetyl residue, thereby blocking PAM of the remaining amines.

Klosterman and co-workers employed *N*-acylation reactions for the PAM of a self-assembled dicopper(II) paddlewheel cage containing endohedral aniline groups.[44] Motivated by the possibility of altering the internal environment of a molecular container, the authors showed that one of the four amines (on average) within cage **36** became acetylated when the complex was treated with acetic anhydride (22 equiv. per cage) in DMF, furnishing cage **37** (Figure 12). The authors rationalized that the

small cavity of **36** could accommodate only a single acetyl group, thereby sterically blocking further acetylation of the remaining amine sites.

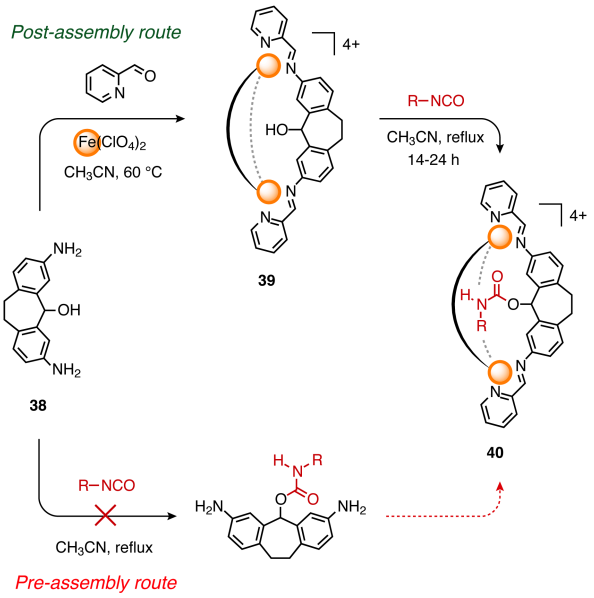

Figure 13. Self-assembly of dibenzosuberol subcomponent **38** with 2-formylpyridine and $Fe(ClO_4)_2$ furnished achiral mesocate **39**, which, when treated with primary isocyanates, gave the corresponding carbamate-modified mesocate (**40**).[45] Subcomponent **38** did not react with primary isocyanates under equivalent conditions, preventing the formation of **40** by pre-assembly means.

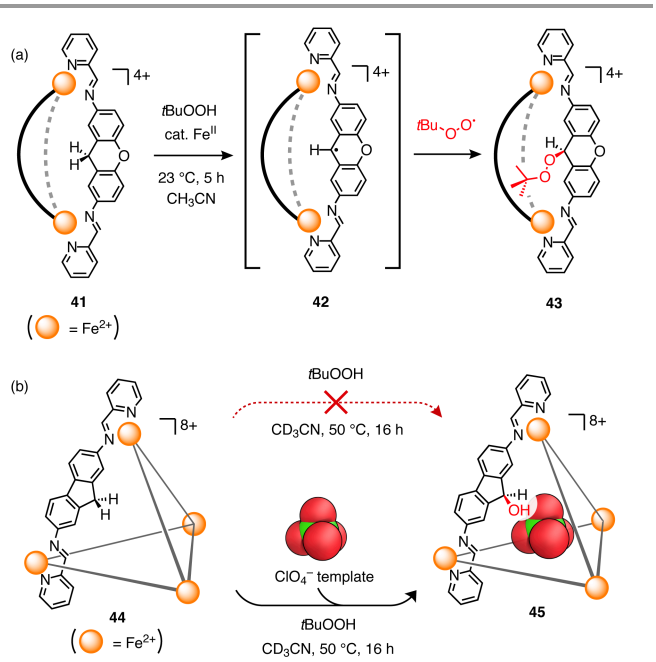

Figure 14. Hooley and co-workers demonstrated post-assembly C–H oxidation of the ligand frameworks of mesocate **41** and tetrahedron **44** using *tert*-butyl hydroperoxide.[46] (a) Oxidation of the xanthene moiety proceeds *via* abstraction of the benzylic hydrogen, catalysed by adventitious Fe^{II}, followed by recombination with $^{\bullet}OOtBu$. Mesocate **43** forms as a single 'all-out' diastereomer to minimise steric hindrance. (b) Oxidation of tetrahedron **44**, which exists as a mixture of diastereomers, can proceed only when a ClO_4^- guest is present within its cavity. In this case, the intermediate fluorene radical combines with $^{\bullet}OH$, generating a single *pseudo*-C_3 diastereomer of **45**.

The examples discussed above demonstrate that complexes featuring substitutionally inert metal coordination bonds (e.g., $N\rightarrow Pt^{II}$ and $O\rightarrow Cu^{II}$) can withstand PAM reactions featuring electrophiles and nucleophiles. By contrast, covalent modification of more dynamic complexes using such reagents presents additional challenges due to the increased likelihood of disrupting their weaker metal-ligand linkages. Hooley and co-workers demonstrated that PAM with nucleophilic/electrophilic reagents can succeed when using self-assembled $Fe^{II}_2L_3$ mesocates based on a tris(2-iminopyridyl)iron(II) coordination motif, which features both labile metal-ligand coordination interactions and dynamic-covalent imine bonds.[45-46] The alcohol groups of dibenzosuberol-edged mesocate **39** reacted with primary and secondary isocyanates, affording carbamate-functionalised mesocates (**40**) (Figure **13**). Interestingly, the free dibenzosuberol subcomponent (**38**) did not react with isocyanates in the same fashion, indicating that carbamoylation only proceeds in the presence of the self-assembled mesocate framework. The authors ascribe the origin of this reactivity to hydrogen bonding between the reactive alcohol groups and an incoming isocyanate electrophile, which accelerates the nucleophilic addition reaction. Consequently, PAM offers a unique route to the functionalised mesocates, since carbamoylation proceeds only on the assembled complex and not its free subcomponents under equivalent reaction conditions.

The relative ease of $Fe^{II}\rightarrow Fe^{III}$ oxidation poses a problem for oxidative PAM reactions involving tris(2-iminopyridyl)iron(II) complexes. However, Hooley and co-workers recently showed that these complexes can undergo clean PAM through diastereoselective radical C–H oxidation reactions.[46] Fe_2L_3 mesocate **41** and $Fe^{II}_4L_6$ tetrahedron **44** are derived from ligands featuring doubly-benzylic methylene bridges (Figure 14). These complexes are amenable to post-assembly benzylic oxidation without appreciable oxidation of the metal centres when treated with *tert*-butyl hydroperoxide (*t*BuOOH, 1.0–1.1 equiv. per benzylic site) in the presence of catalytic Fe^{II}.[47] Interestingly, the outcomes of these PAM reactions differed from analogous oxidations of "free" ligand analogues: while the "free" ligands were oxidised to the corresponding ketones, the complexes underwent only partial oxidation to a peroxide (**43**) or a secondary alcohol (**45**). The authors postulate that oxidation proceeds through initial H atom abstraction at the benzylic position followed by recombination with either $^{\bullet}OOtBu$ or $^{\bullet}OH$. This unusual reactivity is attributed to the geometries of both complexes, which would become strained upon the introduction of an sp^2 centre at their benzylic positions. The radical recombination reaction was diastereoselective, affording single supramolecular diastereomers for both structures. In the case of mesocate **43**, steric hindrance caused the bulky *t*BuOO- groups to adopt an "all-out" configuration. Sterics were also postulated to play a role in the PAM of tetrahedron **44**: $^{\bullet}OOtBu$ was too large to fit within its central cavity, leaving room only for $^{\bullet}OH$. However, the authors also

found that encapsulated ClO_4^- was necessary for the reaction to proceed. This unusual observation highlights a possible mechanism for using entrapped guests to control the outcomes of PAM reactions.

Mukherjee and co-workers also noted an instance where covalent PAM is directly influenced by stereoelectronic constraints imposed by the parent supramolecular complex.[48] Trinuclear barrel-shaped complex **47**, featuring six aldehyde groups, was prepared *via* self-assembly of $Pd(NO_3)_2$ with ditopic imidazole-based ligand **46** (Figure 15). Treatment of **47** with Meldrum's acid (5 equiv. per aldehyde) resulted in PAM of the exposed aldehyde residues *via* Knoevenagel condensation, yielding hexa-functionalised **48** as the only observed reaction product. Remarkably, control experiments in which the Knoevenagel condensation was attempted on the free ligand under similar conditions gave only small amounts (≤11%) of condensation product **49**, indicating that coordination of the imidazole moieties of **46** to Pd^{II} centres increases the reactivity of the aldehyde groups. This observation echoes the hydrogen-bond assisted isocyanate addition phenomenon reported by Hooley and co-workers (*vide supra*).[45]

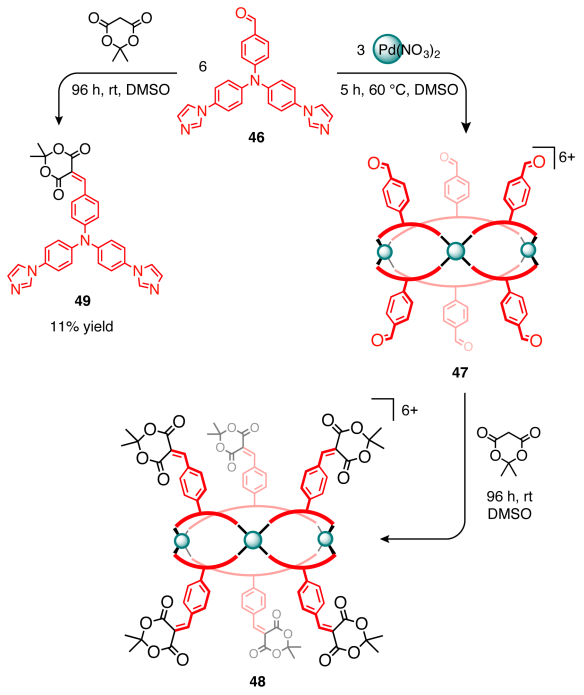

Figure 15. Self-assembly of bis(imidazole) ligand **46** with $Pd(NO_3)_2$ in DMSO afforded trinuclear Pd_3L_6 complex **47**, which features six benzaldehyde moieties decorating the rims of the 'barrel' architecture.[48] Knoevenagel condensation between **47** and Meldrum's acid cleanly furnished hexafunctionalised product **48**. Treatment of ligand **46** with Meldrum's acid under similar conditions gave a low yield of functionalized product **49**.

Yang and co-workers recently succeeded in merging coordination-driven self-assembly with post-assembly polymerisation.[49] The authors envisaged that the broad scope of controlled radical polymerisation—owing to the availability of functional monomers—would generate novel self-assembled materials with new potential applications. Using Stang's organoplatinum(II) metallacycle design,[50] hexagonal cycle **50** was prepared, featuring pendant trithiocarbonate chain-transfer agent moieties capable of reversible addition-fragmentation chain-transfer (RAFT) polymerization.[51] RAFT polymerisation of *N*-isopropylacrylamide (NIPAM) in the presence of **50** afforded water-soluble metallacycle-cored star polymer **51** with an average molecular weight of 50 kDa and moderately narrow molecular weight distribution ($Đ \geq 1.27$). Remarkably, at high concentrations the metallacycle–polymer conjugates formed supramolecular hydrogels, which assembled and disassembled by cooling and heating, or by the addition and abstraction of bromide, which disrupts metal-ligand coordination.

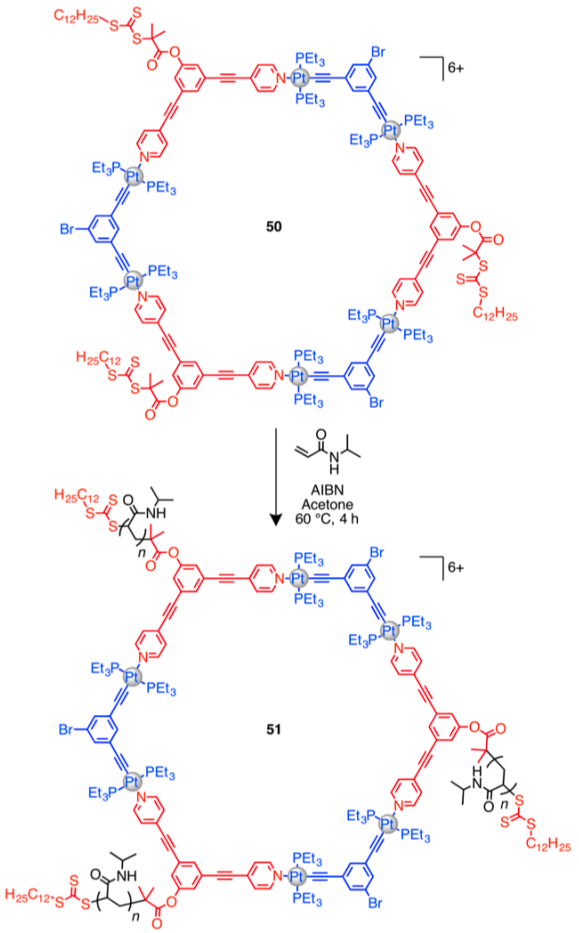

Figure 16. Metallacycle **50** is grafted with three trithiocarbonate RAFT chain-transfer agents, attached to the ligand framework through their carboxylate groups.[49] RAFT polymerisation afforded three-arm metallacycle–polymer conjugate **51** with a molecular mass of approximately 50 kDa and a moderate molecular weight distribution ($Đ \geq 1.27$).

3. PAM locking of metal–organic architectures

A promising and underutilised role of PAM in supramolecular chemistry is the use of covalent bonds to stabilise or 'lock-down' labile or metastable self-assembled complexes. Self-assembly relies on structural error checking *via* the formation and dissociation of dynamic bonds, leading a system to its thermodynamic minimum. However, the dynamic character of these bonds also extends to the resulting assemblies, leading to their decomposition when exposed to reactive chemical species such as coordinating ions, nucleophiles, or electrophiles.

Covalent locking is conceptually related but not equivalent to MPCS (*vide supra*). PAM-locking methods stabilise metallosupramolecular architectures through covalent reactions that preserve their metal–ligand bonds, whereas MPCS may employ the metal centre as a disposable synthetic auxiliary. The stability imparted by covalent locking is therefore important for realising the practical applications of metallosupramolecular complexes, especially in cases where their stability might be challenged by biological milieu or under extreme conditions of pH, temperature and concentration.

Our group developed an approach to PAM-locking during investigations into the self-assembly of trisaniline building block **52**.[52] In the self-assembly of **52** with 2-formylpyridine and $Fe(NTf_2)_2$ (Figure 17), the initial kinetic product of the reaction is $Fe^{II}_2L_3$ triple helicate **53**. However, helicate **53** is metastable and rearranges to form the thermodynamically-favoured $Fe^{II}_4L_4$ face-capped tetrahedron **54** after several days.

We devised a PAM locking strategy that exploits the different metal-to-ligand stoichiometries of complexes **53** and **54** to achieve selective covalent modification. Unlike tetrahedron **54**, in which all three aniline residues on each subcomponent are bound to the metal, helicate **53** only employs two out of three aniline moieties for metal coordination, with the third remaining free. Hence, interception of this third reactive aniline unit with a PAM reaction deprives the ligand of its third coordinating moiety, thus trapping the system at the out-of-equilibrium helicate stage.

Two types of PAM reaction were employed to trap the free aniline: *N*-acylation to give **55** *via* treatment with acid anhydrides or activated esters, and azidation to give **56**. While helicate **53** was not sufficiently stable for further applications, PAM-modified derivatives of kinetically-trapped helicate **55** could be used as a large, rigid threefold-symmetric macroligand for further self-assembly using a Ru^{II}-porphyrin (**57**). Complexation of trisaniline **52** and subsequent PAM also provides an alternative approach to prepare mono-functionalised derivatives of such polyamines, avoiding the usual difficulties of statistical functionalisation or the need to employ protecting groups.

PAM-locking can also be achieved by reinforcing the metal–ligand coordination bonds of a metallosupramolecular complex through additional covalent buttressing around the metal centres. Glasson, Lindoy and co-workers demonstrated an exemplary use of reductive amination to selectively lock-down either $Fe^{II}_2L_3$ complex **59** or $Fe^{II}_4L_6$ complex **60** from an equilibrating solution of quaterpyridyl ligand **58** and $Fe(PF_6)_2$ in CH_3CN (Figure 18).[53] The authors noted that $Fe^{II}_2L_3$ helicate **59** is the kinetic product of self-assembly, being favoured at short reaction times and under dilute conditions, whereas $Fe^{II}_4L_6$ tetrahedron **60** is the thermodynamic product. Once assembled, the architectures can be 'capped' by treating their exposed 5-(*tert*-butyl)benzaldehyde residues with ammonium acetate followed by reduction with sodium cyanoborohydride. The formation of tertiary amine groups locked the complexes in their assembled states (**61** and **62**), rendering them kinetically inert and stable towards perturbations that would cause the non-locked complexes to decompose.

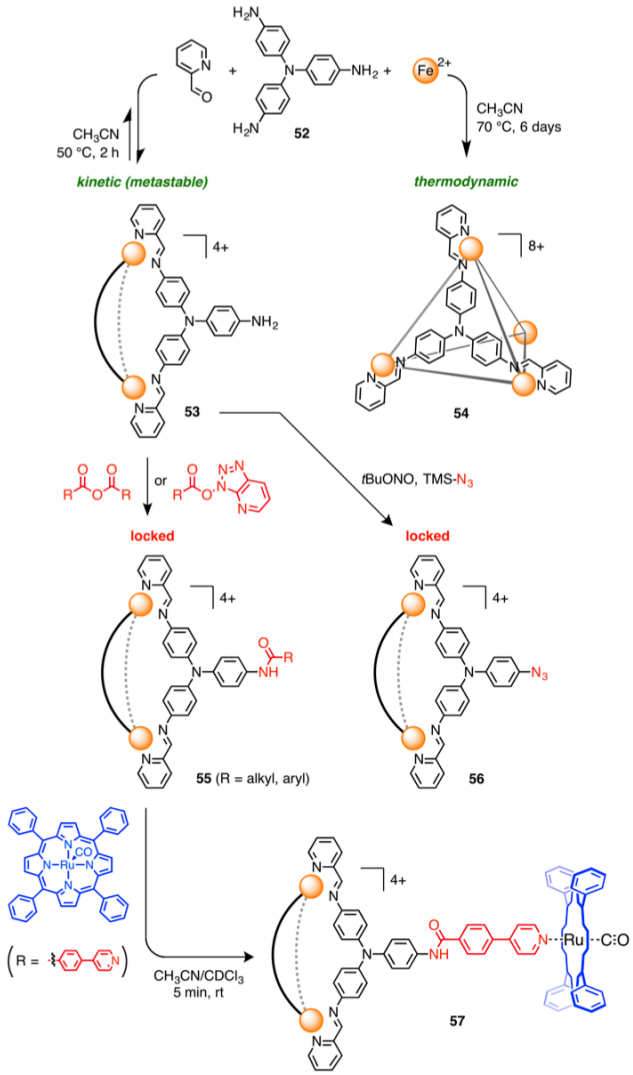

Figure 17. Helicate **53** initially forms as a metastable kinetic product, rearranging to tetrahedron **54** upon prolonged heating.[52] The helicate-to-tetrahedron transformation can be prevented by covalent PAM of the free amine units of **53** through acylation or azidation reactions, leading to out-of-equilibrium triply-functionalised complexes **55** and **56**, respectively. The introduction of ligand moieties onto congeners of **55** enabled further self-assembly reactions, exemplified by the formation of tris(Ru^{II}-porphyrin) complex **57**.

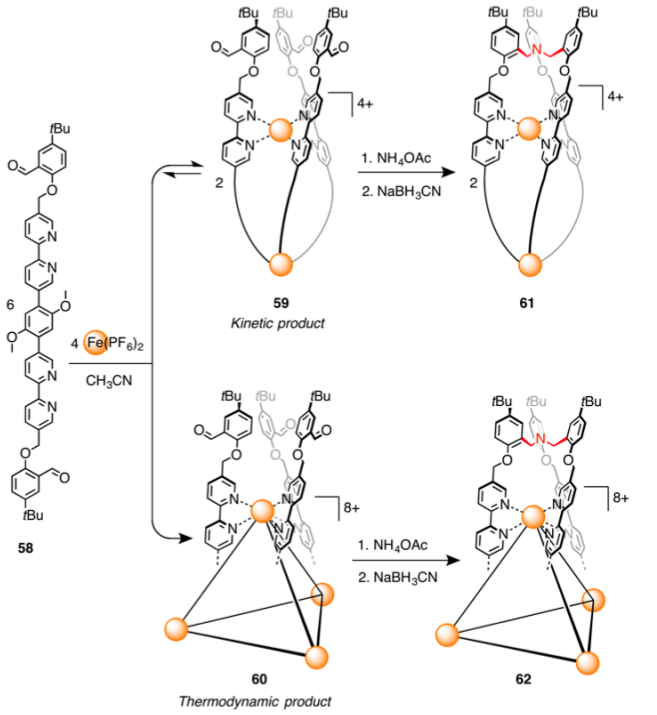

Figure 18. Self-assembly of quaterpyridyl ligand **58** with $Fe(PF_6)_2$ affords either $Fe^{II}_2L_3$ helicate **59** or $Fe^{II}_4L_6$ tetrahedron **60**, depending on concentration and reaction duration.[53] Post-assembly reductive amination of the exposed aldehyde residues at the metal vertices furnished 'locked-down' architectures **61** and **62**, which were rendered non-dynamic by the reductive formation of permanent covalent bonds.

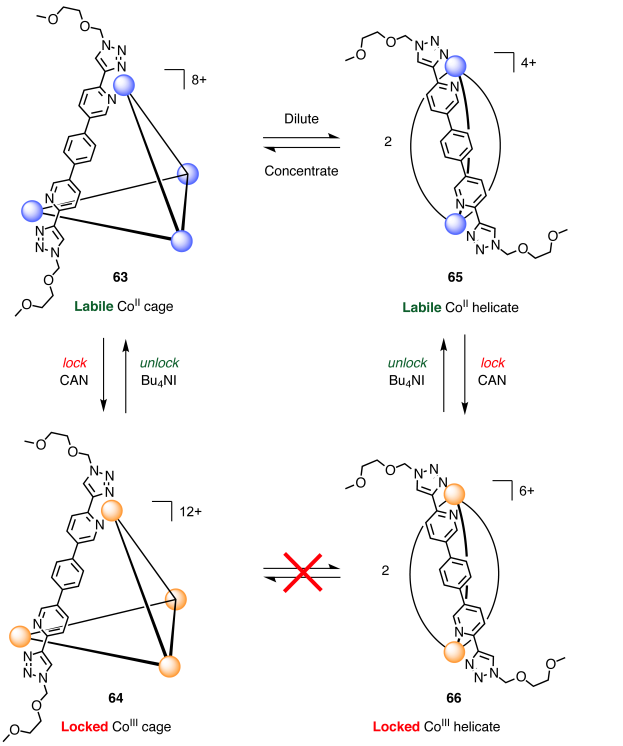

Figure 19. Lusby and co-workers demonstrated post-assembly $Co^{II} \rightarrow Co^{III}$ oxidative locking of tetrahedron **63** to generate **64**.[55] In subsequent work,[56] the same group showed that the product distribution can be fixed from an equilibrating mixture of tetrahedron **63** and helicate **65** through oxidative locking and unlocking. Purple spheres denote Co^{II} centres, and orange spheres denote Co^{III} centres.

The introduction of covalent buttressing around the metal centres is a reliable approach for fortifying labile complexes. However, incorporating reactive functionalities into a ligand can add several steps to its synthesis.[13c] Lusby and co-workers, inspired by the early work of Williams and co-workers,[54] devised an elegant and potentially general solution to this problem by locking down a labile metallosupramolecular complex through post-assembly oxidation of redox-active metal vertices.[55] While no new covalent bonds are introduced in this method, post-assembly oxidation increases the bond strength of the coordinative metal–ligand bonds, thereby rendering the complex kinetically inert. This metal-ligand bond strengthening qualifies post-assembly oxidation as an alternate form of covalent PAM, and a powerful post-assembly locking strategy.

In their study, Lusby and co-workers showed that substitutionally-labile paramagnetic $Co^{II}_4L_6$ tetrahedron **63** was readily oxidised by ceric ammonium nitrate (CAN, 1 equiv. per Co^{II}) to give diamagnetic $Co^{III}_4L_6$ tetrahedron **64** in 97% yield (Figure 19). Oxidation of the Co^{II} centres to Co^{III} rendered the tetrahedron substitutionally inert. The authors demonstrated the utility of their oxidative locking strategy by preparing the water-soluble nitrate salt of **64**. Kinetic fixation of the tetrahedron by oxidation allowed it to encapsulate triisopropylsilanol in a concentrated solution of sodium nitrate (5 M). Such high salt concentrations would compromise the stability of a more labile complex, thus highlighting the ability of this PAM-locking strategy to augment the robustness of metallosupramolecular container molecules.

In follow-up work,[56] Lusby and co-workers employed their oxidative locking strategy to freeze the product distribution of an equilibrating mixture of supramolecular complexes. When synthesised from cobalt(II) perchlorate, $Co^{II}_4L_6$ tetrahedron **63** exists in equilibrium with $Co^{II}_2L_3$ helicate **65**, with the position of equilibrium depending on the concentration of the reaction mixture. Treatment of the Co^{II} helicate–tetrahedron system with CAN (1 equiv. per Co^{II}) resulted in oxidation of the labile Co^{II} centres to inert Co^{III} centres, thereby 'freezing' the equilibrium. The authors also demonstrated that the 'frozen' Co^{III} architectures could be reductively unlocked by the addition of iodide (1 equiv. per Co^{III}), thereby re-establishing the equilibrium between the Co^{II} structures.

The capacity to perform *in situ* oxidative locking and reductive unlocking PAM reactions offers an elegant solution to the trade-off typically encountered between dynamic ligand exchange, which is necessary for structural error-checking during self-assembly, and architectural stability, which requires kinetically inert metal–ligand bonds. One potential limitation of this approach, however, is that it may be restricted to the Co^{II}/Co^{III} redox couple. Future work is likely to focus on expanding the scope of this methodology to other self-assembled architecture types using different redox-active metals.

4. PAM-triggered structural and constitutional transformations

In the examples of PAM derivatisation and locking methods discussed so far, a defining feature of successful PAM is preservation of the intact parent complex. In general, PAM protocols are designed specifically to accommodate the lability of supramolecular complexes and avoid their decomposition. In some cases, however, altering the geometry, sterics or electronics of the ligand framework through PAM can cause the parent complex to undergo a controlled structural or constitutional transformation into another discrete self-assembled architecture. These changes can provide a mechanism for modulating structurally-dependent functions of a complex; for instance, by changing the cavity size of a supramolecular host[57] or by reversibly exposing and blocking catalytic sites incorporated into the ligand framework.[58] More generally, a change in molecular geometry in response to a chemical stimulus can facilitate the transfer of information through mechanical actuation.[59] This behaviour is exemplified in biology by the allosteric conformational changes of haemoglobin during dioxygen binding and release.[60]

Recently, Yang and co-workers provided a comprehensive review of transformations between discrete supramolecular architectures,[61] covering a diverse range of triggering stimuli including solvent exchange, changes in temperature, guest binding and PAM reactions. Extending beyond covalent PAM, their analysis covered a broader range of post-assembly reactions, including ligand and metal addition/exchange reactions and dynamic covalent modifications to the organic building blocks. Here we focus on rarer instances of covalent PAM that alter the ligand framework of an assembled complex to trigger subsequent structural reconfiguration.

The self-assembly behaviour of a ligand is determined primarily by the angular relationships between the coordination vectors of its donor atoms. Consequently, covalent PAM reactions that alter these angular relationships can be used to drive structural transformations. Zhao, Stang, and co-workers demonstrated this principle by performing post-assembly metalation reactions on [6+6] hexagonal macrocycle **67** (Figure 20).[62] The reaction between dicobalt octacarbonyl (1 equiv. per alkyne) and the alkyne linkages within the ligand framework of **67** resulted in a distortion of the pyridyl coordination vectors from 180° to 120°. This change triggered the reorganisation of **67** into a smaller [3+3] hexagon (**68**) to relieve bond-strain introduced by PAM. The authors also demonstrated that the same reaction could be used to trigger transformations of related complexes featuring 1,2-di(pyridin-4-yl)ethyne ligands, illustrating the potential to extend this approach to other two- and three-dimensional assemblies.

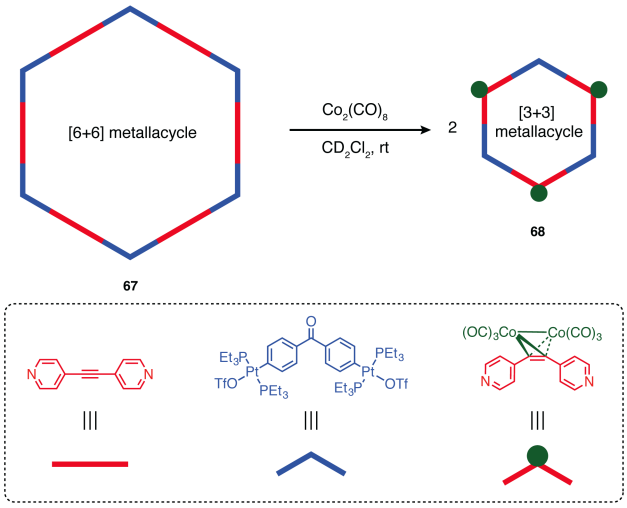

Figure 20. The reaction between dicobalt octacarbonyl (1 equiv. per alkyne) and the alkyne moieties of [6+6] hexagon **67** alters the geometry of the bis(pyridyl) linker (red), triggering a structural reorganization that produces two equivalents of smaller [3+3] hexagon **68**.[62]

Covalent PAM can also activate building block exchange reactions by altering the electronics of a complex's ligand framework. Our group employed this concept as the basis of an autocatalytic system of photooxidation-driven substitution reactions on the framework of a BODIPY-edged $Fe^{II}_4L_6$ tetrahedron.[63] The design of this system exploits the known ability of iminopyridyl-based ligands to undergo *in situ* transamination reactions with more electron-rich 4-substituted anilines. The thermodynamic driving force for this substitution can be quantified by the Hammett parameter, σ_{para}, of the aniline's *para* substituent.[41] Initially the system consists of a mixture of 4-iodoaniline (σ_{para} = 0.18) and tetrahedron **69**, containing 4-(methylthio)aniline (σ_{para} = 0.00) residues (Figure 21). The Hammett parameter of 4-iodoaniline indicates that it is not sufficiently electron-rich to substantially displace the 4-(methylthio)aniline residues from tetrahedron **69**. Nonetheless, a small amount of mixed-aniline tetrahedron **70** forms at equilibrium.

When the system is exposed to light under aerobic conditions, the BODIPY units incorporated into the edges of the tetrahedron generate singlet oxygen *in situ*. This, in turn, oxidises the 4-(methylthio) groups of the aniline residues to the more electron-deficient sulfoxide groups (σ_{para} = 0.49) incorporated into **71**. The resulting 4-(methylsulfinyl)aniline residues are sufficiently electron-poor to be displaced by 4-iodoaniline, the incorporation of which increases the rate of singlet oxygen production through a heavy-atom-induced spin-orbit coupling enhancement. Consequently, the rate of *S*-oxidation, and thus aniline displacement, is accelerated, furnishing iodo-substituted **72** as the final product. Post-assembly oxidation of the ligand building blocks, together with dynamic covalent transamination reactions, thus form a positive feedback loop that leads to an autocatalytic constitutional transformation of a self-assembled complex.

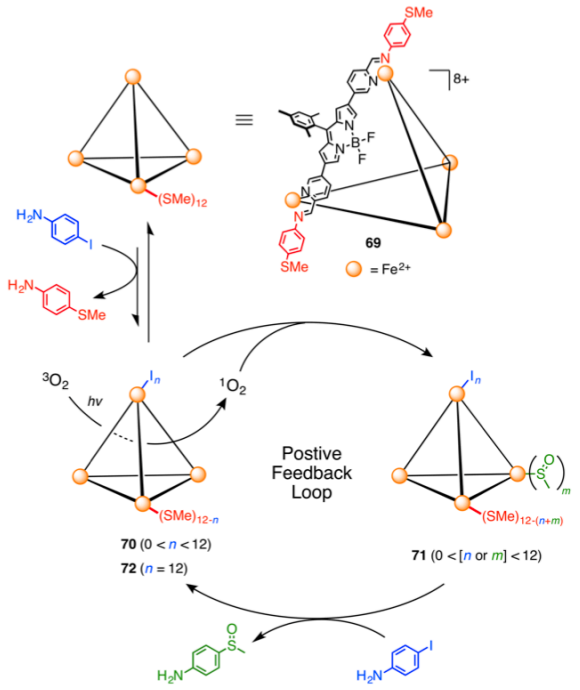

Figure 21. An autocatalytic substitution system consists of BODIPY-edged tetrahedron **69** and 4-iodoaniline in equilibrium with a small amount of mixed-aniline tetrahedron **70**.[63] The BODIPY units sensitize singlet oxygen generation when exposed to light, resulting in post-assembly oxidation of the 4-(methylthio)aniline residues of **70**, which generates a driving force for aniline exchange. Increasing incorporation of iodine atoms into the framework of **70** enhances the rate of singlet oxygen production, which in turn accelerates oxidation and subsequent displacement of the 4-(methylthio)aniline residues.

In addition to constitutional changes, PAM can also engender subtle configurational changes in supramolecular frameworks. Our group designed a PAM-responsive anthracene-edged $Fe^{II}_4L_6$ tetrahedron (**73**) which exploits the normal electron-demand DA reactivity of anthracene derivatives (Figure 22).[64] Cage **73** has idealised *T* point group symmetry, whereby all four Fe^{II} ions within a cage possess the same *Δ* or *Λ* configuration. We anticipated that the structural change resulting from the conversion of a planar anthracene panel to a bent dihydroanthracene during DA reactions would alter the relative energies of the different cage diastereomers, influencing the host–guest properties of the complex. Cage **73** undergoes PAM with tetracyanoethylene (TCNE) to give **74**, which exists as a complex mixture of diastereoisomers due to the DA reactions occurring on both the interior and exterior faces of its anthracene panels. Addition of fullerene C_{60} to **74** leads to the formation of 1:1 host–guest complex $C_{60}\subset$**74**. Single crystal X-ray diffraction analysis revealed that the binding of C_{60} promoted reconfiguration of **74** to a *T*-symmetric configuration with all TCNE residues situated on the cage exterior to accommodate the C_{60} guest. Modified cage **74** also encapsulates $[Co(C_2B_9H_{11})_2]^-$, which does not bind in parent cage **73**. This highlights the capacity of PAM to optimise host–guest interactions.

Intriguingly, the addition of C_{60} to parent cage **73** produces adduct **75**, which arose from direct DA cycloaddition between encapsulated C_{60} and three anthracene ligands sharing an apical vertex of the cage. X-ray crystallography showed that three double bonds of the fullerene had reacted with the central ring of each anthracene unit in an overall orthogonal (*e*,*e*,*e*)-tris-relationship to each other. The DA reaction with C_{60} also led to reconfiguration of the cage from a homochiral *T*-configuration to a heterochiral structure of idealised C_3 symmetry in which the apical Fe^{II} centre is of opposite handedness to the three basal Fe^{II} centres. The three unmodified anthracene moieties in **75** could undergo further PAM with TCNE to give cage **76**, which also possessed C_3 symmetry. Hence, PAM in this case could both induce configurational changes of this complex and control its guest binding behaviour.

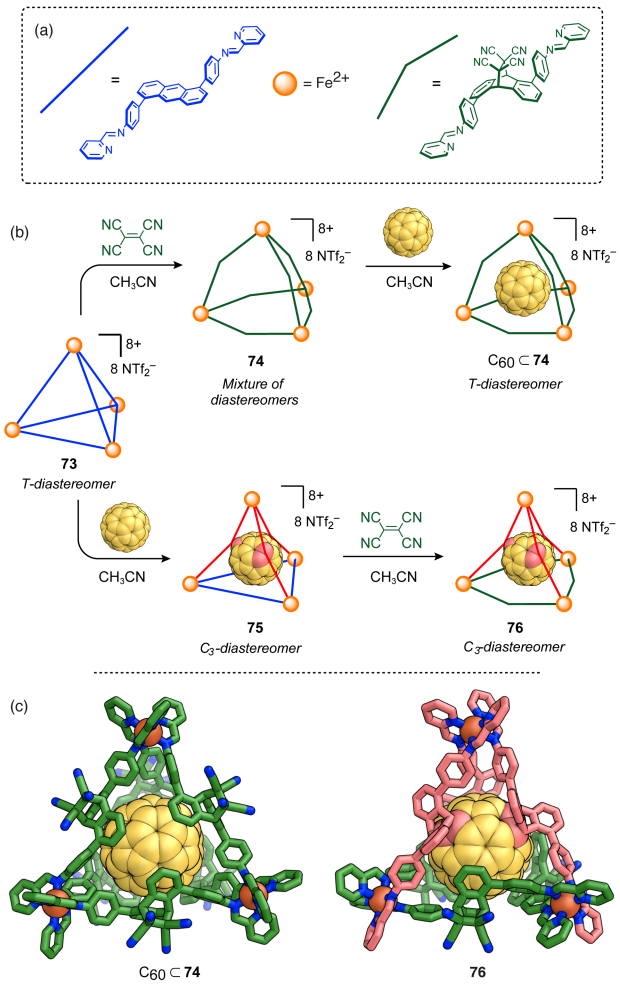

Figure 22. PAM of anthracene-panelled **73** by DA reactions alters its interactions with guests.[64] (a) Representations of the building block configurations in cages **73**–**76**. (b) *T*-symmetric cage **73** undergoes PAM with tetracyanoethylene (TCNE) to give **74** as a mixture of diastereomers. The binding of fullerene C_{60} causes a stereochemical reconfiguration to give the *T*-diastereomer as $C_{60}\subset$**74**. Conversely cage **73** undergoes PAM with C_{60} directly, giving C_3-diastereomer **75**. This adduct undergoes further PAM with TCNE on its remaining sites to give **76**. (c) X-ray crystal structures of $C_{60}\subset$**74** and **76**.

Photochemical cyclisation reactions offer a strategy for achieving reversible covalent PAM, and consequently reversible structural transformations, of supramolecular complexes. In this area, the photocyclisation of dithienylethene (DTE) derivatives developed by Irie and co-workers[65] is especially

notable. DTEs can undergo electrocyclic transitions between ring-open and ring-closed forms, with each state exhibiting different optical and electronic properties (Figure 23, top). The photostability of DTEs also endows them with resistance to fatigue, allowing these compounds to undergo many ring-opening and closing cycles. Importantly, neither the ring-open nor the ring-closed states undergo thermal relaxation: conversion in either direction is triggered only by the absorption of light at a specific wavelength.

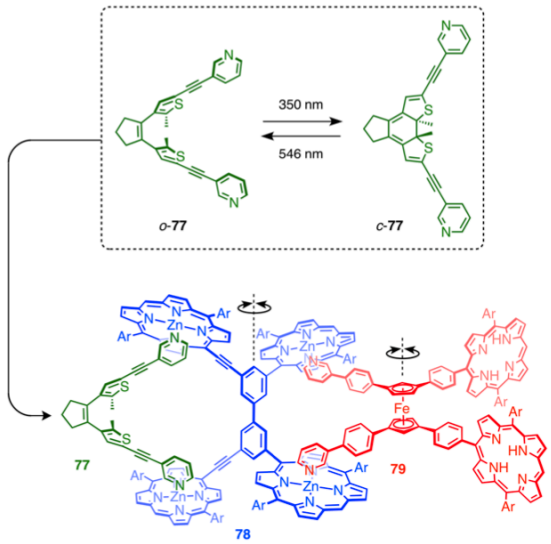

Figure 23. The self-assembly of photo-switch **77**, tetraporphyrin hinge **78** and chiral scissoring unit **79** forms a light-mediated molecular 'tweezer'.[66] Irradiation of the DTE chromophore in **77** with UV or visible light drives electrocyclic transitions between open (*o*-**77**) and closed (*c*-**77**) configurations. Light-driven changes in the geometry of the photosensitive component are transmitted *via* bridge **78** to subunit **79**, which produces a chiroptical response.

In 2008, Aida and co-workers demonstrated long-distance mechanical communication in a self-assembled complex using a DTE photo-switch for mechanical actuation.[66] Their signal-transmission system consisted of a self-assembled ternary complex comprised of three moveable components: an initial photochromic DTE photo-switch (**77**), an intermediate tetraporphyrinatozinc(II) hinge (**78**), and a terminal chiral "scissoring" output unit (**79**) (Figure 23). These three units are connected to each other through ditopic porphyrinatozinc(II)–pyridine coordination interactions. Upon exposure of the ternary complex to UV light (λ = 350 nm), the DTE unit undergoes photocyclisation, altering the angle between the pyridyl groups of **77**. The carefully-designed connectivity of the ternary complex enables transmission of this structural change through a concerted 'scissoring' action between the subunits, producing changes in the circular dichroism spectrum of unit **79**. Exposure to green light (λ = 546 nm) restored the complex to its original state.

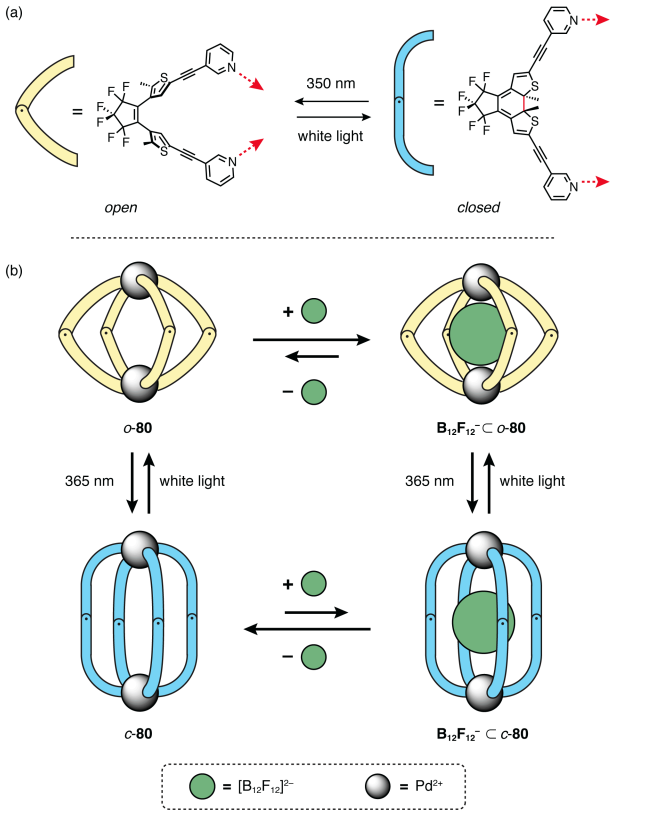

Figure 24. Self-assembled Pd_2L_4 cage **80**, which features ligands containing photochromic DTE units.[67] (a) Representations of the DTE-containing ligands in complex **80**. Light absorption drives the interconversion between an 'open' flexible state and a rigid 'closed' state. (b) The difference in cavity size between the open-DTE and closed-DTE forms of **80** resulted in differential binding of dodecafluorododecaborate (green circle).

Inspired by reports of 2D supramolecular assemblies incorporating light-switchable motifs,[67] Clever and co-workers reported the first use of light-switchable elements in a self-assembled 3D coordination cage.[68] Based on previous cage designs from their group,[57a] the authors prepared Pd_2L_4 complex **80** (Figure 24). The complex contains two square-planar Pd^{II} ions and four bis-monodentate pyridyl ligands, each containing a perfluorinated dithienylethene (DTE) photo-switch. Irradiation with UV (365 nm) or white light caused the cage to interconvert between a conformationally-flexible ring-open form (*o*-**80**) and a rigid ring-closed form (c-**80**), respectively.

DOSY NMR experiments revealed that *o*-**80** (r_h = 7.04 Å) is smaller than *c*-**80** (r_h = 8.67 Å), which the authors explain in terms of the flexibility of the ligand framework in the open form, leading to a more condensed structure. The authors also demonstrated that the open and closed forms of cage **80** bound dodecafluorododecaborate with different affinities, with *o*-**80** exhibiting a stronger preference for the guest. They proposed that the flexibility of *o*-**80** allows the cage to better accommodate the guest, whereas *c*-**80** is too rigid to adapt its structure. Photo-switching between the open and closed forms was found to operate in the presence of the guest, making it possible to dynamically alter the proportion of bound guest within the system through light stimulation.

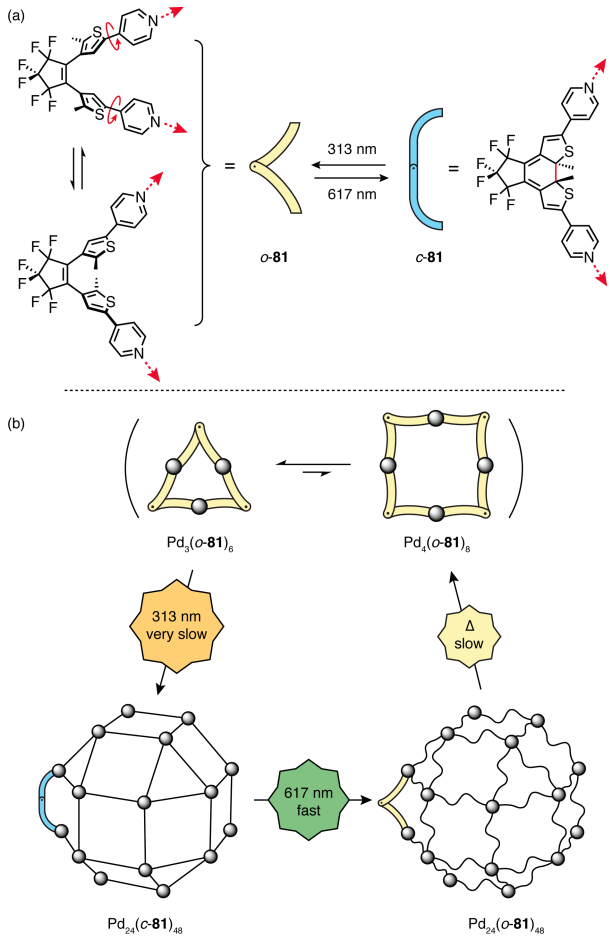

Figure 25. Photochemical PAM drives structural interconversions between 2D and 3D assemblies reported by Clever and co-workers.[69] (a) Representations of DTE-containing ligand **81**, which interconverts between ring open (*o*-**81**) and closed (*c*-**81**) forms upon absorption of different wavelengths of light. (b) Self-assembly of DTE-containing ligand **81** with Pd^{II} furnished 2D polygonal assembles $Pd_3(o\text{-}\mathbf{81})_6$ and $Pd_4(o\text{-}\mathbf{81})_8$ when the DTE unit was in its ring-open state (*o*-**81**). When in its ring-closed state (*c*-**81**), the geometry of the DTE units favoured a larger 3D rhombicuboctahedron, $Pd_{24}(c\text{-}\mathbf{81})_{48}$. Irradiation of the DTE chromophore at different wavelengths changed the relative orientations of the pyridyl donors, leading to the structural transformations.

More recently, Clever and co-workers employed a similar photo-switchable ligand strategy to bring about major transformations between 2D and 3D supramolecular architectures.[69] Assembly of bis(pyridyl) DTE ligand *o*-**81** with Pd^{II} in a 2:1 ratio afforded a mixture of $Pd_3(o\text{-}\mathbf{81})_6$ and $Pd_4(o\text{-}\mathbf{81})_8$ metallacycles (Figure 25). The authors rationalised the presence of both structures based upon the flexibility of the open form of the DTE unit, which leads to only small energy differences between the triangular and square assemblies. Irradiation converted the ligands to their more rigid ring-closed form, with the resulting strain causing the 2D structures to disassemble and rearrange completely into a much larger 3D $Pd_{24}(c\text{-}\mathbf{81})_{48}$ rhombicuboctahedron. Irradiation of the rhombicuboctahedron with visible light reconverted the DTE units back to their open form, producing a metastable $Pd_{24}(o\text{-}\mathbf{81})_{48}$ structure, which relaxed back to the entropically-favoured 2D metallacycles through dissociation and reformation of the Pd^{II}–pyridine bonds. This ground-breaking work on the incorporation of the DTE photo-switch into a 3D metallosupramolecular complex will undoubtedly inspire more widespread use of this robust light-sensitive motif for triggering controlled supramolecular shape transformations.

Conclusions and Future Perspectives

The development of covalent PAM strategies in metallosupramolecular chemistry continues to offer new approaches for generating architectures with tailored functionalities. While future work on PAM will undoubtedly see the application of new covalent bond-forming reactions to supramolecular contexts, there are underexplored areas that warrant more immediate research. For instance, recent progress has highlighted how PAM locking procedures are a promising way to improve the robustness of metallosupramolecular assemblies. This topic remains relatively unexplored, with locking procedures successfully demonstrated only using M_2L_3 helicates and M_4L_6 tetrahedra to date.[52-53, 56] There is a need for more general methods to lock larger, more complex and fragile architectures, especially those whose practical applications are limited by poor stability.

The use of reversible PAM reactions to trigger structural transformations can allow self-assembled complexes to dynamically adapt their structures—and thus, functions—in response to applied stimuli. Future work on PAM-triggered shape transformations might see the continued development of supramolecular *systems* that employ several distinct stimulus types—including covalent PAM—to drive structural transformations. Conceivably, each distinct stimulus type (e.g., covalent PAM, guest binding, or ligand exchange) could be linked to a specific structural transformation such that the system expresses a supramolecular product specific to that stimulus.

Several authors have shown that low-symmetry metallosupramolecular architectures[70] can engender anisotropic functions such as chiral catalysis,[71] energy transfer,[72] and recognition of low-symmetry guest molecules.[73] While low-symmetry architectures are typically accessed through heteroleptic self-assembly,[74] combinations of covalent PAM reactions—especially those serving derivatisation, rearrangement and locking roles—could offer alternative routes for introducing asymmetry.

Our group has recently shown that complex supramolecular systems—in this case, a reaction cascade leading to signal transduction—can be constructed from the existing PAM toolbox.[42] Several reviews[2g, 61] have highlighted supramolecular cascades as an area of growing interest for developing novel guest recognition[75] and catalytic systems.[76] PAM-based cascade reactions provide a new tool for constructing complex supramolecular networks, which may mimic some of the complex functions of biological systems. For these same reasons, covalent PAM might also gain a foothold in the design of new supramolecular logic gates[77] and feedback mechanisms in future work.

PAM has far-reaching implications for accessing non-thermodynamic products of self-assembly reactions (i.e.,

kinetically trapped states), as well as fixing and altering the product distributions of supramolecular systems *in situ*. Understanding the interplay between *de novo* assembly and PAM is critical to developing functional and responsive self-assembled materials. Covalent PAM thus offers a powerful and growing set of tools for the construction of bespoke architectures and functional supramolecular systems that will underpin new technological applications.

Conflicts of Interests

There are no conflicts to declare.

Acknowledgements

D.A.R. acknowledges the Gates Cambridge Trust. B.S.P. acknowledges the Royal Commission for the Exhibition of 1851 Research Fellowship and the Fellowship from Corpus Christi College, Cambridge. This work was also supported by the UK Engineering and Physical Sciences Research Council (EPSRC, EP/P027067/1) and the European Research Council (695009). The authors thank A. Danos for proofreading the manuscript.

Notes and references

1. (a) D. L. Caulder and K. N. Raymond, *Acc. Chem. Res.*, 1999, **32**, 975-982; (b) D. L. Caulder and K. N. Raymond, *J. Chem. Soc., Dalton Trans.*, 1999, 1185-1200; (c) R. Chakrabarty, P. S. Mukherjee and P. J. Stang, *Chem. Rev.*, 2011, **111**, 6810-6918; (d) T. K. Ronson, S. Zarra, S. P. Black and J. R. Nitschke, *Chem. Commun.*, 2013, **49**, 2476-2490; (e) M. M. J. Smulders, I. A. Riddell, C. Browne and J. R. Nitschke, *Chem. Soc. Rev.*, 2013, **42**, 1728-1754; (f) L. Chen, Q. Chen, M. Wu, F. Jiang and M. Hong, *Acc. Chem. Res.*, 2015, **48**, 201-210; (g) Z. He, W. Jiang and C. A. Schalley, *Chem. Soc. Rev.*, 2015, **44**, 779-789.
2. (a) S. R. Seidel and P. J. Stang, *Acc. Chem. Res.*, 2002, **35**, 972-983; (b) N. C. Gianneschi, M. S. Masar and C. A. Mirkin, *Acc. Chem. Res.*, 2005, **38**, 825-837; (c) G. R. Whittell, M. D. Hager, U. S. Schubert and I. Manners, *Nat. Mater.*, 2011, **10**, 176-188; (d) P. D. Frischmann, K. Mahata and F. Wurthner, *Chem. Soc. Rev.*, 2013, **42**, 1847-1870; (e) J. G. Hardy, *Chem. Soc. Rev.*, 2013, **42**, 7881-7899; (f) X. Su and I. Aprahamian, *Chem. Soc. Rev.*, 2014, **43**, 1963-1981; (g) S. Zarra, D. M. Wood, D. A. Roberts and J. R. Nitschke, *Chem. Soc. Rev.*, 2015, **44**, 419-432; (h) M. Castellano, R. Ruiz-García, J. Cano, J. Ferrando-Soria, E. Pardo, F. R. Fortea-Pérez, S.-E. Stiriba, W. P. Barros, H. O. Stumpf, L. Cañadillas-Delgado, J. Pasán, C. Ruiz-Pérez, G. de Munno, D. Armentano, Y. Journaux, F. Lloret and M. Julve, *Coord. Chem. Rev.*, 2015, **303**, 110-138; (i) C. Garcia-Simon, M. Costas and X. Ribas, *Chem. Soc. Rev.*, 2016, **45**, 40-62; (j) K. Y. Zhang, S. Liu, Q. Zhao and W. Huang, *Coord. Chem. Rev.*, 2016, **319**, 180-195.
3. C. T. Walsh, *Posttranslational Modification of Proteins: Expanding Nature's Inventory*, Roberts & Co, 2005.
4. A. D. Goldberg, C. D. Allis and E. Bernstein, *Cell*, 2007, **128**, 635-638.
5. (a) K. Hansson and J. Stenflo, *J. Thromb. Haemost.*, 2005, **3**, 2633-2648; (b) Y. L. Deribe, T. Pawson and I. Dikic, *Nat. Struct. Mol. Biol.*, 2010, **17**, 666-672; (c) Y.-C. Wang, S. E. Peterson and J. F. Loring, *Cell Res.*, 2014, **24**, 143-160; (d) N. T. Snider and M. B. Omary, *Nat. Rev. Mol. Cell Biol.*, 2014, **15**, 163-177; (e) G. Duan and D. Walther, *PLoS Comput. Biol.*, 2015, **11**, e1004049.
6. (a) M. A. Gauthier, M. I. Gibson and H.-A. Klok, *Angew. Chem. Int. Ed.*, 2009, **48**, 48-58; (b) D. J. Hall, H. M. Van Den Berghe and A. P. Dove, *Polym. Int.*, 2011, **60**, 1149-1157; (c) H. Durmaz, A. Sanyal, G. Hizal and U. Tunca, *Polym. Chem.*, 2012, **3**, 825-835; (d) C. J. Galvin and J. Genzer, *Prog. Polym. Sci.*, 2012, **37**, 871-906; (e) S. Tempelaar, L. Mespouille, O. Coulembier, P. Dubois and A. P. Dove, *Chem. Soc. Rev.*, 2013, **42**, 1312-1336; (f) K. A. Günay, P. Theato and H.-A. Klok, *J. Polym. Sci., Part A: Polym. Chem.*, 2013, **51**, 1-28; (g) Q. Li and Z. Li, *Polym. Chem.*, 2015, **6**, 6770-6791.
7. (a) S. J. Garibay, Z. Wang, K. K. Tanabe and S. M. Cohen, *Inorg. Chem.*, 2009, **48**, 7341-7349; (b) K. K. Tanabe and S. M. Cohen, *Chem. Soc. Rev.*, 2011, **40**, 498-519; (c) J. Jiang, Y. Zhao and O. M. Yaghi, *J. Am. Chem. Soc.*, 2016, **138**, 3255-3265; (d) B. Gui, X. Meng, H. Xu and C. Wang, *Chin. J. Chem.*, 2016, **34**, 186-190; (e) S. M. Cohen, *J. Am. Chem. Soc.*, 2017, **139**, 2855-2863; (f) T. Islamoglu, S. Goswami, Z. Li, A. J. Howarth, O. K. Farha and J. T. Hupp, *Acc. Chem. Res.*, 2017, **50**, 805-813.
8. (a) Y. Du, K. Mao, P. Kamakoti, P. Ravikovitch, C. Paur, S. Cundy, Q. Li and D. Calabro, *Chem. Commun.*, 2012, **48**, 4606-4608; (b) M. Calik, T. Sick, M. Dogru, M. Döblinger, S. Datz, H. Budde, A. Hartschuh, F. Auras and T. Bein, *J. Am. Chem. Soc.*, 2016, **138**, 1234-1239; (c) M. S. Lohse, T. Stassin, G. Naudin, S. Wuttke, R. Ameloot, D. De Vos, D. D. Medina and T. Bein, *Chem. Mater.*, 2016, **28**, 626-631; (d) P. J. Waller, S. J. Lyle, T. M. Osborn Popp, C. S. Diercks, J. A. Reimer and O. M. Yaghi, *J. Am. Chem. Soc.*, 2016, **138**, 15519-15522; (e) C. S. Diercks and O. M. Yaghi, *Science*, 2017, **355**, eaal1585; (f) S. Mitra, H. S. Sasmal, T. Kundu, S. Kandambeth, K. Illath, D. Díaz Díaz and R. Banerjee, *J. Am. Chem. Soc.*, 2017, **139**, 4513-4520; (g) Q. Sun, B. Aguila, J. Perman, L. D. Earl, C. W. Abney, Y. Cheng, H. Wei, N. Nguyen, L. Wojtas and S. Ma, *J. Am. Chem. Soc.*, 2017, **139**, 2786-2793.
9. A. F. Williams, C. Piguet and G. Bernardinelli, *Angew. Chem. Int. Ed.*, 1991, **30**, 1490-1492.
10. (a) C. R. Becer, R. Hoogenboom and U. S. Schubert, *Angew. Chem. Int. Ed.*, 2009, **48**, 4900-4908; (b) M. G. Finn and V. V. Fokin, *Chem. Soc. Rev.*, 2010, **39**, 1231-1232.
11. (a) C. O. Dietrich-Buchecker, J. P. Sauvage and J. M. Kern, *J. Am. Chem. Soc.*, 1984, **106**, 3043-3045; (b) C. O. Dietrich-Buchecker and J. P. Sauvage, *Chem. Rev.*, 1987, **87**, 795-810; (c) J.-P. Sauvage, *Angew. Chem. Int. Ed.*, 2017, **56**, 11080-11093.
12. (a) J. D. Crowley, S. M. Goldup, A.-L. Lee, D. A. Leigh and R. T. McBurney, *Chem. Soc. Rev.*, 2009, **38**, 1530-1541; (b) C. D. Meyer, C. S. Joiner and J. F. Stoddart, *Chem. Soc. Rev.*, 2007, **36**, 1705-1723; (c) J.-F. Ayme, J. E. Beves, C. J. Campbell and D. A. Leigh, *Chem. Soc. Rev.*, 2013, **42**, 1700-1712; (d) J. E. M. Lewis, P. D. Beer, S. J. Loeb and S. M. Goldup, *Chem. Soc. Rev.*, 2017, **46**, 2577-2591.
13. (a) S. J. Rowan, S. J. Cantrill, G. R. L. Cousins, J. K. M. Sanders and J. F. Stoddart, *Angew. Chem. Int. Ed.*, 2002, **41**, 898-952; (b) P. T. Corbett, J. Leclaire, L. Vial, K. R. West, J.-L. Wietor, J. K. M. Sanders and S. Otto, *Chem. Rev.*, 2006, **106**, 3652-3711; (c) J. A. Thomas, *Chem. Soc. Rev.*, 2007, **36**, 856-868; (d) Y. Jin, C. Yu, R. J. Denman and W. Zhang, *Chem. Soc. Rev.*, 2013, **42**, 6634-6654; (e) A. M. Castilla, W. J. Ramsay and J. R. Nitschke, *Acc. Chem. Res.*, 2014, **47**, 2063-2073.
14. C. O. Dietrich-Buchecker, J. P. Sauvage and J. P. Kintzinger, *Tetrahedron Lett.*, 1983, **24**, 5095-5098.
15. (a) J.-P. Collin, C. Dietrich-Buchecker, P. Gaviña, M. C. Jimenez-Molero and J.-P. Sauvage, *Acc. Chem. Res.*, 2001, **34**, 477-487; (b) K. S. Chichak, S. J. Cantrill, A. R. Pease, S.-H. Chiu, G. W. V. Cave,

J. L. Atwood and J. F. Stoddart, *Science*, 2004, **304**, 1308-1312; (c) J. E. Beves, B. A. Blight, C. J. Campbell, D. A. Leigh and R. T. McBurney, *Angew. Chem. Int. Ed.*, 2011, **50**, 9260-9327; (d) J.-F. Ayme, J. E. Beves, D. A. Leigh, R. T. McBurney, K. Rissanen and D. Schultz, *Nat. Chem.*, 2012, **4**, 15-20; (e) C. S. Wood, T. K. Ronson, A. M. Belenguer, J. J. Holstein and J. R. Nitschke, *Nat. Chem.*, 2015, **7**, 354-358.

16. J. Guo, P. C. Mayers, G. A. Breault and C. A. Hunter, *Nat. Chem.*, 2010, **2**, 218-222.
17. (a) D. G. Hamilton, N. Feeder, S. J. Teat and J. K. M. Sanders, *New J. Chem.*, 1998, **22**, 1019-1021; (b) T. J. Kidd, D. A. Leigh and A. J. Wilson, *J. Am. Chem. Soc.*, 1999, **121**, 1599-1600.
18. D. A. Leigh, R. G. Pritchard and A. J. Stephens, *Nat. Chem.*, 2014, **6**, 978-982.
19. V. Marcos, A. J. Stephens, J. Jaramillo-Garcia, A. L. Nussbaumer, S. L. Woltering, A. Valero, J.-F. Lemonnier, I. J. Vitorica-Yrezabal and D. A. Leigh, *Science*, 2016, **352**, 1555-1559.
20. J. J. Danon, A. Krüger, D. A. Leigh, J.-F. Lemonnier, A. J. Stephens, I. J. Vitorica-Yrezabal and S. L. Woltering, *Science*, 2017, **355**, 159-162.
21. M. C. O'Sullivan, J. K. Sprafke, D. V. Kondratuk, C. Rinfray, T. D. W. Claridge, A. Saywell, M. O. Blunt, J. N. O'Shea, P. H. Beton, M. Malfois and H. L. Anderson, *Nature*, 2011, **469**, 72-75.
22. D. V. Kondratuk, L. M. A. Perdigão, A. M. S. Esmail, J. N. O'Shea, P. H. Beton and H. L. Anderson, *Nat. Chem.*, 2015, **7**, 317-322.
23. N. Kamonsutthipaijit and H. L. Anderson, *Chem. Sci.*, 2017, **8**, 2729-2740.
24. P. Neuhaus, A. Cnossen, J. Q. Gong, L. M. Herz and H. L. Anderson, *Angew. Chem. Int. Ed.*, 2015, **54**, 7344-7348.
25. (a) V. Aucagne, J. Berná, J. D. Crowley, S. M. Goldup, K. D. Hänni, D. A. Leigh, P. J. Lusby, V. E. Ronaldson, A. M. Z. Slawin, A. Viterisi and D. B. Walker, *J. Am. Chem. Soc.*, 2007, **129**, 11950-11963; (b) J. Berná, J. D. Crowley, S. M. Goldup, K. D. Hänni, A.-L. Lee and D. A. Leigh, *Angew. Chem. Int. Ed.*, 2007, **46**, 5709-5713; (c) S. M. Goldup, D. A. Leigh, T. Long, P. R. McGonigal, M. D. Symes and J. Wu, *J. Am. Chem. Soc.*, 2009, **131**, 15924-15929; (d) J. D. Crowley, S. M. Goldup, N. D. Gowans, D. A. Leigh, V. E. Ronaldson and A. M. Z. Slawin, *J. Am. Chem. Soc.*, 2010, **132**, 6243-6248; (e) S. M. Goldup, D. A. Leigh, P. R. McGonigal, V. E. Ronaldson and A. M. Z. Slawin, *J. Am. Chem. Soc.*, 2010, **132**, 315-320; (f) P. E. Barran, H. L. Cole, S. M. Goldup, D. A. Leigh, P. R. McGonigal, M. D. Symes, J. Wu and M. Zengerle, *Angew. Chem. Int. Ed.*, 2011, **50**, 12280-12284; (g) H. Lahlali, K. Jobe, M. Watkinson and S. M. Goldup, *Angew. Chem. Int. Ed.*, 2011, **50**, 4151-4155.
26. M. Denis and S. M. Goldup, *Nat. Rev. Chem.*, 2017, **1**, 0061.
27. D. Zhao, S. Tan, D. Yuan, W. Lu, Y. H. Rezenom, H. Jiang, L.-Q. Wang and H.-C. Zhou, *Adv. Mater.*, 2011, **23**, 90-93.
28. J. J. Low, A. I. Benin, P. Jakubczak, J. F. Abrahamian, S. A. Faheem and R. R. Willis, *J. Am. Chem. Soc.*, 2009, **131**, 15834-15842.
29. (a) S. Han, Z. Ma, R. Hopson, Y. Wei, D. Budil, S. Gulla and B. Moulton, *Inorg. Chem. Commun.*, 2012, **15**, 78-83; (b) Z. Ma, S. Han, R. Hopson, Y. Wei and B. Moulton, *Inorg. Chim. Acta*, 2012, **388**, 135-139.
30. Z. Li, T. S. Seo and J. Ju, *Tetrahedron Lett.*, 2004, **45**, 3143-3146.
31. D. C. Kennedy, C. S. McKay, M. C. B. Legault, D. C. Danielson, J. A. Blake, A. F. Pegoraro, A. Stolow, Z. Mester and J. P. Pezacki, *J. Am. Chem. Soc.*, 2011, **133**, 17993-18001.
32. J. Dommerholt, F. P. J. T. Rutjes and F. L. van Delft, *Top. Curr. Chem.*, 2016, **374**, 16.
33. N. J. Agard, J. A. Prescher and C. R. Bertozzi, *J. Am. Chem. Soc.*, 2004, **126**, 15046-15047.
34. R. Chakrabarty and P. J. Stang, *J. Am. Chem. Soc.*, 2012, **134**, 14738-14741.
35. (a) M. Tominaga, K. Suzuki, M. Kawano, T. Kusukawa, T. Ozeki, S. Sakamoto, K. Yamaguchi and M. Fujita, *Angew. Chem. Int. Ed.*, 2004, **43**, 5621-5625; (b) Q.-F. Sun, S. Sato and M. Fujita, *Nat. Chem.*, 2012, **4**, 330-333; (c) X. Yan, T. R. Cook, P. Wang, F. Huang and P. J. Stang, *Nat. Chem.*, 2015, **7**, 342-348.
36. (a) R. A. A. Foster and M. C. Willis, *Chem. Soc. Rev.*, 2013, **42**, 63-76; (b) A.-C. Knall and C. Slugovc, *Chem. Soc. Rev.*, 2013, **42**, 5131-5142.
37. (a) I. A. Barker, D. J. Hall, C. F. Hansell, F. E. Du Prez, R. K. O'Reilly and A. P. Dove, *Macromol. Rapid Commun.*, 2011, **32**, 1362-1366; (b) C. F. Hansell, P. Espeel, M. M. Stamenović, I. A. Barker, A. P. Dove, F. E. Du Prez and R. K. O'Reilly, *J. Am. Chem. Soc.*, 2011, **133**, 13828-13831; (c) R. M. Desai, S. T. Koshy, S. A. Hilderbrand, D. J. Mooney and N. S. Joshi, *Biomaterials*, 2015, **50**, 30-37; (d) S. Jain, K. Neumann, Y. Zhang, J. Geng and M. Bradley, *Macromolecules*, 2016, **49**, 5438-5443.
38. (a) C. Chen, C. A. Allen and S. M. Cohen, *Inorg. Chem.*, 2011, **50**, 10534-10536; (b) J. E. Clements, J. R. Price, S. M. Neville and C. J. Kepert, *Angew. Chem. Int. Ed.*, 2014, **53**, 10164-10168.
39. (a) M. L. Blackman, M. Royzen and J. M. Fox, *J. Am. Chem. Soc.*, 2008, **130**, 13518-13519; (b) M. F. Debets, J. C. M. van Hest and F. P. J. T. Rutjes, *Org. Biomol. Chem.*, 2013, **11**, 6439-6455; (c) T. Reiner and B. M. Zeglis, *J. Labelled Compd. Radiopharm.*, 2014, **57**, 285-290; (d) Y. Gong and L. Pan, *Tetrahedron Lett.*, 2015, **56**, 2123-2132; (e) Z. Ni, L. Zhou, X. Li, J. Zhang and S. Dong, *PLOS ONE*, 2015, **10**, e0141918; (f) I. Nikić, J. H. Kang, G. E. Girona, I. V. Aramburu and E. A. Lemke, *Nat. Protocols*, 2015, **10**, 780-791.
40. D. A. Roberts, B. S. Pilgrim, J. D. Cooper, T. K. Ronson, S. Zarra and J. R. Nitschke, *J. Am. Chem. Soc.*, 2015, **137**, 10068-10071.
41. C. Hansch, A. Leo and R. W. Taft, *Chem. Rev.*, 1991, **91**, 165-195.
42. B. S. Pilgrim, D. A. Roberts, T. G. Lohr, T. K. Ronson and J. R. Nitschke, *Nat. Chem.*, 2017, DOI: 10.1038/nchem.2839.
43. M. Wang, W.-J. Lan, Y.-R. Zheng, T. R. Cook, H. S. White and P. J. Stang, *J. Am. Chem. Soc.*, 2011, **133**, 10752-10755.
44. V. Brega, M. Zeller, Y. He, H. Peter Lu and J. K. Klosterman, *Chem. Commun.*, 2015, **51**, 5077-5080.
45. M. C. Young, A. M. Johnson and R. J. Hooley, *Chem. Commun.*, 2014, **50**, 1378-1380.
46. L. R. Holloway, P. M. Bogie, Y. Lyon, R. R. Julian and R. J. Hooley, *Inorg. Chem.*, 2017, DOI: 10.1021/acs.inorgchem.1027b01958.
47. A. Rabion, d. S. Chen, J. Wang, R. M. Buchanan, J.-L. Seris and R. H. Fish, *J. Am. Chem. Soc.*, 1995, **117**, 12356-12357.
48. D. Samanta, A. Chowdhury and P. S. Mukherjee, *Inorg. Chem.*, 2016, **55**, 1562-1568.
49. W. Zheng, L.-J. Chen, G. Yang, B. Sun, X. Wang, B. Jiang, G.-Q. Yin, L. Zhang, X. Li, M. Liu, G. Chen and H.-B. Yang, *J. Am. Chem. Soc.*, 2016, **138**, 4927-4937.
50. J. B. Pollock, T. R. Cook and P. J. Stang, *J. Am. Chem. Soc.*, 2012, **134**, 10607-10620.
51. J. Chiefari, Y. K. Chong, F. Ercole, J. Krstina, J. Jeffery, T. P. T. Le, R. T. A. Mayadunne, G. F. Meijs, C. L. Moad, G. Moad, E. Rizzardo and S. H. Thang, *Macromolecules*, 1998, **31**, 5559-5562.
52. D. A. Roberts, A. M. Castilla, T. K. Ronson and J. R. Nitschke, *J. Am. Chem. Soc.*, 2014, **136**, 8201-8204.
53. C. R. K. Glasson, G. V. Meehan, M. Davies, C. A. Motti, J. K. Clegg and L. F. Lindoy, *Inorg. Chem.*, 2015, **54**, 6986-6992.
54. L. J. Charbonniere, G. Bernardinelli, C. Piguet, A. M. Sargeson and A. F. Williams, *J. Chem. Soc., Chem. Commun.*, 1994, 1419-1420.

55. P. R. Symmers, M. J. Burke, D. P. August, P. I. T. Thomson, G. S. Nichol, M. R. Warren, C. J. Campbell and P. J. Lusby, *Chem. Sci.*, 2015, **6**, 756-760.
56. M. J. Burke, G. S. Nichol and P. J. Lusby, *J. Am. Chem. Soc.*, 2016, **138**, 9308-9315.
57. (a) S. Freye, J. Hey, A. Torras-Galán, D. Stalke, R. Herbst-Irmer, M. John and G. H. Clever, *Angew. Chem. Int. Ed.*, 2012, **51**, 2191-2194; (b) M. Frank, J. Hey, I. Balcioglu, Y.-S. Chen, D. Stalke, T. Suenobu, S. Fukuzumi, H. Frauendorf and G. H. Clever, *Angew. Chem. Int. Ed.*, 2013, **52**, 10102-10106.
58. (a) N. C. Gianneschi, S. T. Nguyen and C. A. Mirkin, *J. Am. Chem. Soc.*, 2005, **127**, 1644-1645; (b) P. A. Ulmann, A. B. Braunschweig, O.-S. Lee, M. J. Wiester, G. C. Schatz and C. A. Mirkin, *Chem. Commun.*, 2009, 5121-5123; (c) H. J. Yoon, J. Kuwabara, J.-H. Kim and C. A. Mirkin, *Science*, 2010, **330**, 66-69; (d) J. Mendez-Arroyo, J. Barroso-Flores, A. M. Lifschitz, A. A. Sarjeant, C. L. Stern and C. A. Mirkin, *J. Am. Chem. Soc.*, 2014, **136**, 10340-10348; (e) A. M. Lifschitz, M. S. Rosen, C. M. McGuirk and C. A. Mirkin, *J. Am. Chem. Soc.*, 2015, **137**, 7252-7261.
59. (a) A. R. Pease, J. O. Jeppesen, J. F. Stoddart, Y. Luo, C. P. Collier and J. R. Heath, *Acc. Chem. Res.*, 2001, **34**, 433-444; (b) C. G. Oliveri, P. A. Ulmann, M. J. Wiester and C. A. Mirkin, *Acc. Chem. Res.*, 2008, **41**, 1618-1629; (c) C. J. Bruns and J. F. Stoddart, *Acc. Chem. Res.*, 2014, **47**, 2186-2199; (d) S. Erbas-Cakmak, D. A. Leigh, C. T. McTernan and A. L. Nussbaumer, *Chem. Rev.*, 2015, **115**, 10081-10206.
60. (a) M. F. Perutz, *Nature*, 1970, **228**, 726-734; (b) A. Bellelli and M. Brunori, *Biochim. Biophys. Acta*, 2011, **1807**, 1262-1272.
61. W. Wang, Y.-X. Wang and H.-B. Yang, *Chem. Soc. Rev.*, 2016, **45**, 2656-2693.
62. L. Zhao, B. H. Northrop and P. J. Stang, *J. Am. Chem. Soc.*, 2008, **130**, 11886-11888.
63. P. P. Neelakandan, A. Jiménez, J. D. Thoburn and J. R. Nitschke, *Angew. Chem. Int. Ed.*, 2015, **54**, 14378-14382.
64. T. K. Ronson, B. S. Pilgrim and J. R. Nitschke, *J. Am. Chem. Soc.*, 2016, **138**, 10417-10420.
65. (a) M. Irie, *Chem. Rev.*, 2000, **100**, 1685-1716; (b) M. Irie, T. Fukaminato, K. Matsuda and S. Kobatake, *Chem. Rev.*, 2014, **114**, 12174-12277.
66. H. Kai, S. Nara, K. Kinbara and T. Aida, *J. Am. Chem. Soc.*, 2008, **130**, 6725-6727.
67. (a) R. Reuter, N. Hostettler, M. Neuburger and H. A. Wegner, *Eur. J. Org. Chem.*, 2009, **2009**, 5647-5652; (b) S. Chen, L.-J. Chen, H.-B. Yang, H. Tian and W. Zhu, *J. Am. Chem. Soc.*, 2012, **134**, 13596-13599; (c) N. Iwasawa, H. Takahagi, K. Ono, K. Fujii and H. Uekusa, *Chem. Commun.*, 2012, **48**, 7477-7479.
68. M. Han, R. Michel, B. He, Y.-S. Chen, D. Stalke, M. John and G. H. Clever, *Angew. Chem. Int. Ed.*, 2013, **52**, 1319-1323.
69. M. Han, Y. Luo, B. Damaschke, L. Gómez, X. Ribas, A. Jose, P. Peretzki, M. Seibt and G. H. Clever, *Angew. Chem. Int. Ed.*, 2016, **55**, 445-449.
70. N. Takashi, U. Hitoshi and S. Mitsuhiko, *Chem. Lett.*, 2013, **42**, 328-334.
71. (a) M. J. Wiester, P. A. Ulmann and C. A. Mirkin, *Angew. Chem. Int. Ed.*, 2011, **50**, 114-137; (b) J. Beswick, V. Blanco, G. De Bo, D. A. Leigh, U. Lewandowska, B. Lewandowski and K. Mishiro, *Chem. Sci.*, 2015, **6**, 140-143; (c) L.-J. Chen, H.-B. Yang and M. Shionoya, *Chem. Soc. Rev.*, 2017, **46**, 2555-2576.
72. (a) M.-S. Choi, T. Yamazaki, I. Yamazaki and T. Aida, *Angew. Chem. Int. Ed.*, 2004, **43**, 150-158; (b) Y. Kobuke, *Eur. J. Inorg. Chem.*, 2006, **2006**, 2333-2351; (c) M. Schmittel, R. S. K. Kishore and J. W. Bats, *Org. Biomol. Chem.*, 2007, **5**, 78-86; (d) M. E. Gallina, B. Baytekin, C. Schalley and P. Ceroni, *Chem. Eur. J.*, 2012, **18**, 1528-1535; (e) M. D. Ward and P. R. Raithby, *Chem. Soc. Rev.*, 2013, **42**, 1619-1636.
73. (a) Q.-Q. Wang, V. W. Day and K. Bowman-James, *Chem. Sci.*, 2011, **2**, 1735-1738; (b) C. Roche, A. Sour and J.-P. Sauvage, *Chem. Eur. J.*, 2012, **18**, 8366-8376; (c) R. Custelcean, *Chem. Commun.*, 2013, **49**, 2173-2182; (d) T. Nakamura, H. Ube, M. Shiro and M. Shionoya, *Angew. Chem. Int. Ed.*, 2013, **52**, 720-723; (e) Q.-Q. Wang, V. W. Day and K. Bowman-James, *J. Am. Chem. Soc.*, 2013, **135**, 392-399; (f) P. A. Gale, N. Busschaert, C. J. E. Haynes, L. E. Karagiannidis and I. L. Kirby, *Chem. Soc. Rev.*, 2014, **43**, 205-241.
74. S. De, K. Mahata and M. Schmittel, *Chem. Soc. Rev.*, 2010, **39**, 1555-1575.
75. (a) E. V. Anslyn, *J. Am. Chem. Soc.*, 2010, **132**, 15833-15835; (b) M. M. J. Smulders, S. Zarra and J. R. Nitschke, *J. Am. Chem. Soc.*, 2013, **135**, 7039-7046; (c) G. Men, C. Chen, C. Liang, W. Han and S. Jiang, *Analyst*, 2015, **140**, 5454-5458.
76. (a) A. G. Salles, S. Zarra, R. M. Turner and J. R. Nitschke, *J. Am. Chem. Soc.*, 2013, **135**, 19143-19146; (b) Z. J. Wang, K. N. Clary, R. G. Bergman, K. N. Raymond and F. D. Toste, *Nat. Chem.*, 2013, **5**, 100-103.
77. (a) A. P. de Silva, S. Uchiyama, T. P. Vance and B. Wannalerse, *Coord. Chem. Rev.*, 2007, **251**, 1623-1632; (b) M. Ikeda, T. Tanida, T. Yoshii, K. Kurotani, S. Onogi, K. Urayama and I. Hamachi, *Nat. Chem.*, 2014, **6**, 511-518.

